

**ANALYSIS OF HEPATIC GENE EXPRESSION IN CHICKENS
WITH HORMONALLY-INDUCED LEAN AND FAT PHENOTYPES**

by

Jessica Ann Hall

A thesis submitted to the Faculty of the University of Delaware in partial fulfillment of the requirements for the degree of Honors Bachelor of Science in Animal Science with Distinction.

Spring 2006

Copyright 2006 Jessica Ann Hall
All Rights Reserved

**ANALYSIS OF HEPATIC GENE EXPRESSION IN CHICKENS
WITH HORMONALLY-INDUCED LEAN AND FAT PHENOTYPES**

by

Jessica Ann Hallxx

Approved: _____
Larry A. Cogburn, Ph.D.
Professor in charge of thesis on behalf of the Advisory Committee

Approved: _____
Carl Schmidt, Ph.D.
Committee member from the Department of Animal and Food Sciences

Approved: _____
Judith Hough-Goldstein, Ph.D.
Committee member from the Board of Senior Thesis Readers

Approved: _____
John Courtright, Ph.D.
Director, University Honors Program

ACKNOWLEDGMENTS

I would like to thank Larry A. Coghurn for his continued guidance and support throughout the entirety of this project. Also, I would like to thank Carl Schmidt and Judith Hough-Goldstein as my second and third readers. I greatly acknowledge the help of Robert J. Tempelman (biostatistics), Fiona McCarthy (gene ontology), and Nares Trakooljul for help in analyses. Furthermore, special thanks to the Science and Engineering Scholars program (2004), the Life Sciences Scholar Program (2005), and the Undergraduate Research Program. The genomics tools and reagents used in this study were developed by the *Consortium for Functional Genomics in Chickens* supported by the USDA-IFAFS Animal Genome Program (Grant # 00-52100-9614). This research was supported by a USDA Training Grant (Grant # 2004-38411-14734) and by grants to LAC from the USDA-IFAFS Animal Genome Program (Grant # 00-52100-9614) and USDA NRI (Grant # 2005-35206-15288).

3.6	Identification of a Novel Obesity-Related Gene Family	54
Discussion	56
4.1	Phenotypic Response to Exogenous Hormones	56
4.2	Transcriptional Response to Exogenous Hormones.....	60
4.3	Clustering Differentially Expressed Genes into Functional Pathways.....	61
4.4	Real-Time qRT-PCR Verification of Obesity-Related Genes	63
4.4.1	Transport Proteins	63
4.4.2	Transcription Factors.....	65
4.4.3	Metabolic Enzymes	66
4.5	Avian β -Defensin: Its Evolutionary Role and Implication in Obesity.....	69
Conclusions	79
Reference List	78

LIST OF TABLES

Table 2.1	Experimental design. Number of birds per treatment and age (days) at end of treatment duration are indicated.	14
Table 2.2	Primers used for real-time qRT-PCR.	25
Table 3.1	Differentially expressed hepatic genes by treatment contrast.	33
Table 3.2	Cellular and regulatory processes involving the differentially expressed hepatic genes between treatment comparisons of CS and T ₃	40
Table 3.3	Metabolic processes involving the differentially expressed hepatic genes in the CS versus T ₃ contrast	43
Table 3.4	Select differentially expressed genes revealed by microarray analysis and verified by real-time qRT-PCR.....	47
Table 3.5	Differentially expressed β -defensin genes from microarray	55

LIST OF FIGURES

Figure 1.1	Phenotypic response to chronic infusion of hormones (2 weeks).....	10
Figure 3.1	Elevation of circulating hormone levels with infusion of exogenous hormones	28
Figure 3.2	Final body weight (A.) and total feed intake (B.) of chickens after acute hormonal treatment	29
Figure 3.3	Plasma metabolite response to infusion of exogenous hormones	31
Figure 3.4	Venn diagram showing three major gene clusters that were either up- or down-regulated with CS, T ₃ , or CS+T ₃ treatment as compared to vehicle control, respectively	33
Figure 3.5	Hierarchical Clustering (GeneSpring) of genes (Y-axis), treatments (VC, CS, T ₃ , or CS+T ₃) and thier biological replications (X-axis).....	36
Figure 3.6	<i>(Legend appears on next page.)</i>	37
Figure 3.6	<i>(Continued from previous page)</i> Pie Charts of the three major gene ontology (GO) categories of differentially expressed hepatic genes.....	38
Figure 3.7	Gene association network of cellular and regulatory processes involved in the response of hepatic genes to either CS or T ₃	42
Figure 3.8	Gene association network of metabolic processes involved in the response of hepatic genes to either CS or T ₃	44
Figure 3.9	Expression of CS-responsive genes as indicated through real-time qRT-PCR.....	48
Figure 3.10	Expression of T ₃ -responsive genes as indicated through real-time qRT-PCR.....	49

Figure 3.11	Expression of key <i>lipogenic</i> genes as indicated through real-time qRT-PCR.....	50
Figure 3.12	Expression of key <i>lipolytic</i> genes as indicated through real-time qRT-PCR.....	51
Figure 3.13	<i>(Legend appears at top of next page.)</i>	53
Figure 3.13	<i>(On the previous page.)</i> Impact of exogenous hormones on key metabolic genes involved in metabolism and synthesis of fat	54
Figure 3.14	Expression of β -defensin 9 as indicated through real-time qRT-PCR	55
Figure 4.1	Phylogenetic relationship of vertebrate β -defensins, with chicken β -defensins on GGA3 highlighted in yellow.	75

ABSTRACT

Obesity is a growing health concern in the United States and has been linked to a global epidemic—the metabolic syndrome. The purpose of this project was to use microarray analysis to unravel the genetic circuits controlling deposition and metabolism of fat in a hormonally-induced obesity model. Glucose, triglyceride, and free fatty acid levels of four-week-old chickens were dramatically altered after acute infusion (six days) of exogenous corticosterone (CS), effectively producing a fat phenotype. A lean phenotype was induced by thyroid hormone (T_3), and the interaction of both hormones (CS+ T_3) was also examined. The Del-Mar 14K Chicken Integrated Systems Microarray (Geo Platform GPL1731) was used to identify differentially expressed hepatic genes (false discovery rate, $P < 0.05$). In the contrast of fat (CS) and lean (T_3) phenotypes, 231 genes were up-regulated by CS, whereas 532 genes were up-regulated by T_3 . This study revealed several transport proteins, transcription factors, and metabolic enzymes that control lipogenic (CS induced) and lipolytic (T_3 induced) pathways. Also, the divergent expression of three genes belonging to the β -defensin family (*DEFB9*, *DEFB10*, and *DEFB11*) suggests a novel role for these antimicrobial peptides in adiposity. This project provides new insight into genetic control of metabolic disorders, such as diabetes and obesity. (Supported by USDA Training Grant # 2004-38411-14734, USDA-IFAFS Animal Genome Program Grant # 00-52100-9614, and USDA NRI Grant # 2005-35206-15288.)

Chapter 1

INTRODUCTION

1.1 Obesity and the Metabolic Syndrome

Obesity is a major health concern in the United States, where about two thirds of the population are overweight (1). Being overweight has many deleterious effects on health. As the prevalence for obesity has increased, a relationship between abdominal obesity and insulin resistance has brought global attention to a common metabolic disorder known as the ‘metabolic syndrome’ or ‘syndrome X’ (2). This disorder includes the symptoms of glucose intolerance, abdominal (visceral) obesity, hypertension, and dyslipidemia, and puts patients at a major risk for coronary heart disease and other cardiovascular complications. Heart disease remains the leading cause of death in industrialized nations, totaling 28% of the deaths in the United States in 2002 (3). With the trend of obesity on the rise, the associated complications are expected to parallel its occurrence until preventative measures are introduced to thwart this global health epidemic.

1.1.1 Insulin Resistance, a Problem and Contradiction

The dominant risk factor present in the metabolic syndrome is insulin resistance. Insulin resistance, simply stated, is when the body’s tissues cannot respond normally to insulin. This leads to other metabolic abnormalities, such as obesity and type 2 diabetes. However, the maintenance of obesity requires a

sensitivity to insulin's lipogenic action, making the role of insulin resistance in obesity rather counterintuitive. In normal functioning cells, insulin causes appropriate transport proteins to bind to the cell membrane, thereby allowing glucose to enter the cell. In addition to facilitating glucose metabolism, insulin also induces production of lipogenic transcription factors, which cause increased expression of key enzymes involved in lipogenesis. Thus, 'insulin resistance,' as it applies to the metabolic syndrome, refers to resistance to insulin-stimulated glucose uptake and not to an inhibition of insulin-stimulated lipogenesis (1). Unger (1) suggests that insulin's paradoxical nature emanates from the response to protect against lipid-induced cytotoxicity by limiting excess cellular glucose, the main source of *de novo* lipogenesis. As the concentration of fatty acids increase, insulin resistance is induced to reduce glucose transport and subsequent glucose oxidation. Thus, to counter the health problems related to insulin resistance, new approaches to reduce obesity must be explored (4).

1.1.2 A Genetic Approach

There are a number of factors that contribute to obesity (genetics, nutrition, hormone balance, lifestyle, etc.). Accordingly, there is a growing body of evidence demonstrating the influence of genetics on the metabolic syndrome (2). In an extensive review of obesity-related publications, Perusse et al.(5) report the status of the human obesity gene map and list some of the purported genetic contributors to this global health problem. However, the authors acknowledge the potential for error in their listing, which necessitates the need for further studies to identify the genes that contribute to an increased risk in obesity. Despite progress over the past decade in our understanding of the relationship between obesity and the metabolic syndrome (2), its

molecular mechanisms still require deeper understanding. In order to circumvent this potentially life-threatening condition and impede the current obesity epidemic, further research is urgently needed on the genes and metabolic pathways involved in the development of metabolic diseases (2;3;6;7). Through the use of genetic models, insight into obesity and its treatment will hopefully be reached.

1.2 The Chicken as a Model System

Since the days of Aristotle, the chick has endured a prominent history as a favored experimental model in developmental biology (8;9). Although extensively employed in questions pertaining to embryology and immunology, its ability to serve as a system for the understanding of human disease raised initial skepticism. Mammals and birds have innumerable differences that separate them physiologically, so metabolic pathways or other genetic inferences made with avian models raise concern for their practical application to human medicine. Critiques focused on these limitations and deterred chicken-enthusiast scientists from tackling questions of human pathology with chicken-based research. However, in the last half-decade, the importance of the chicken as a model has re-entered the spotlight (9). With the advent of new technical progress in molecular biology, the chicken's sophisticated power as a model in functional genomics has been affirmed.

1.2.1 Advances in Avian Genomics

Comparative functional genomics owes its foundation to the use of animal models to illuminate the complexities of human biological systems, including metabolic disease. Due to recent advancements in avian genomics (i.e., a completed genome sequence, expressed sequence tags, and microarrays), the chicken (*Gallus*

gallus) has gained the status as a model research organism (10). Published by a consortium in 2004, the 6.6× coverage draft sequencing and initial analysis of the chicken genome made the chicken the first agricultural animal to have its DNA sequenced (11). The distinctive karotype of the chicken consists of 1.2×10^9 DNA base pairs, which are organized into 1 pair of sex chromosomes and 38 pairs of autosomes. Unlike the human genome, its autosomes take on a range of sizes, with the eight largest autosomes identified as macrochromosomes and the remaining smaller autosomes identified as microchromosomes (11). Another important difference is that the chicken genome is about one-third the size of the average mammalian genome. This is due largely to a reduction in the number of sequence repeats and duplicated gene copies in the avian genome sequence (11).

1.2.1.1 Conserved Syntenic Relationship

The evolutionary position of the chicken with respect to other vertebrates provides an organism that is related distantly enough to humans to enable the comparison of conserved functionally important genes. With the completion of the human genome in 2003, scientists have been eager to relate stretches of decoded sequence to their transcriptional regulation and functional elements (12). Comparison of chicken and human genomes reveals 70 million DNA base pairs (bp) in common, suggesting genetic material has been conserved since the two species split from a common ancestor approximately 310 million years ago (12). Thus, the chicken occupies a convenient outgroup that will undoubtedly illuminate important shared derived and shared primitive characters that distinguish avian and mammalian biology.

Given the remarkable level of conservation in genetic coding, an understanding of molecular mechanisms in animal models will provide an understanding of these mechanisms in humans. The level of similarity between syntenic arrangements in the chicken and human genome is astonishingly high and indicates an extensive conservation in gene order between these two species (13). About 85% of the chicken and human orthologous genes are on segments of orthologous chromosomes, meaning that the majority of genes in the chicken that share similar sequences and functions to human genes are present in the chicken genome at similar locations to their position in the human genome (11). This is due to the slow rate of interchromosomal rearrangements since the evolutionary split of chickens from mammals. In contrast, rearrangements of gene sequences as to their chromosomal location are much higher in the lineage that has led to the present-day mouse model. To date, evidence confirms that the human genome's arrangement of genes is more closely related to chickens than to mice (11;13). The conserved syntenic relationship between human and chicken genomes makes the chicken an invaluable tool to understanding the vital metabolic pathways that have been conserved throughout evolutionary time.

1.2.1.2 A Comprehensive Catalog of Chicken ESTs

In addition to the revelations brought forth through the completed chicken genome sequence, the dramatic increase in the number of chicken expressed sequence tags (ESTs) have also aided in the elevation of the chicken to model organism status. The importance of an EST catalog cannot be over stressed, as each EST is a unique cDNA fragment within the coding region of a gene and is of great use in identifying a full-length gene. Before 2001, only a few thousand chicken ESTs were available in

public databases (10). As of April 2006, the number of chicken ESTs entered in the NCBI dbEST division of GenBank (http://www.ncbi.nlm.nih.gov/dbEST/dbEST_summary.html) has grown to 588,231, placing *Gallus gallus* twelfth on the species dbEST list. These chicken EST contigs have helped advance the construction of microarrays (14), making the analysis of global gene expression of the chicken possible.

1.2.1.3 Development of High-Density Chicken cDNA Microarrays

All chicken ESTs found in public databases as of March 1, 2003 (approximately 407 thousand) were assembled with the CAP3 fragment assembly program (15) into 33,949 high-fidelity contigs that could represent the number of *bona fide* genes expressed in the chicken (16). This allowed Larry A. Cogburn and colleagues to develop and print both tissue-specific and systems-wide chicken cDNA microarrays under a USDA-IFAFS consortium project (17). A prototype liver-specific array (3.1K unigenes) was printed on nylon membranes and used in several preliminary studies (18-20). The Chicken Metabolic/Somatic and Neuroendocrine Systems Microarrays were also printed and used as prototype microarrays on glass slides (10;21). Recently, they have combined both of these systems-wide gene sets into the Del-Mar 14K Chicken Integrated Systems Microarray (Geo Platform GPL1731) (10). This universal high density microarray enables the exploration of gene expression on a genomic scale from a variety of metabolic tissues and is a powerful tool in identifying major metabolic pathways.

1.2.2 Agricultural and Biomedical Relevance of the Chicken

The last fifty years of intensive artificial selection further enhance the chicken's importance as a model organism. Poultry producers, breeding for specific traits in their domestic chicken populations, have directed evolution toward distinctive polymorphisms associated with qualitative traits (12). Many of these production traits have been mapped to quantitative trait loci (QTL) and are important not only to agriculture, but to human medicine, as well. For example, through the analysis of divergently-selected lines of fat and lean chickens, major fatness QTL have been identified on chicken chromosomes (GGA) 1, 4 and 5 (21-24). In poultry production, a goal of the producer is to grow lean birds without a lot of excess fat. Understanding the genetic contribution to fatness versus leanness enables the production of a leaner food source, which, in turn, contributes toward a healthier human population. In addition, this same knowledge can be applied toward human medicine to further a greater understanding of the genetic underpinnings of obesity. Thus, its agricultural and biomedical applications reveal the double impact that a chicken model can have on benefiting global health.

1.3 Induced Obesity in Avian Models

One way of observing the molecular contributions to obesity is to examine models that are inherently obese or non-obese (i.e. divergently-selected fat and lean lines of chickens). Cogburn et al. has also examined the effect of metabolic perturbations—the embryo-to-hatching transition (25) and the fasting and re-feeding response (20)—in an attempt to elucidate the genetic pathways involved in fat metabolism. Both models have contributed to a better understanding of lipogenesis in chickens, albeit with limited clarity. A third type of perturbation study involves

endocrine manipulation of the adrenotropic (corticosterone) and thyrotropic (thyroid hormone) axes. This model capitalizes on hormones with known endogenous functions to induce phenotypic changes similar to the obese pathology.

1.3.1 Hormonal Manipulation Affects Phenotype

There has been growing interest in the role of glucocorticoids on insulin resistance and subsequent obesity. Wang (26) provides an analysis implicating this relationship, which necessitates the need for further study of glucocorticoid action on the metabolic syndrome. The major glucocorticoid found in birds is corticosterone (CS), which is a hormone produced by the adrenal cortex in response to stress. Work by Saadoun et al. (27) has linked the effects of corticosterone to insulin resistance and fat metabolism in the chicken through studies on divergently-selected lines of fat and lean chickens. Furthermore, Simon (28) has shown how the lipogenic action of exogenous corticosterone can cause insulin resistance and alter the metabolic utilization of nutrients to favor fat deposition at the expense of muscle deposition. However, the metabolic and regulatory mechanisms governing these changes remain poorly understood in chickens (10;29).

In additional studies of hormonal perturbation, manipulation of the thyroid axis helped in the discovery of potential metabolic gene networks related to obesity. The metabolically-active thyroid hormone, tri-iodothyronine (T_3), acts to increase the overall metabolic activity of the entire body by adjusting the ratio of insulin-to-glucagon (I/G) in the plasma. The I/G molar ratio is indicative of an animal's metabolic state and appears to play an important role in the determination of fat accretion. A high I/G molar ratio correlates to increased lipogenesis and deposition of body fat, whereas a low I/G molar ratio favors lipolysis and catabolism of body fat.

Studies by Cogburn et al. have shown that chickens with a low level of dietary T₃ experience a decreased I/G molar ratio and subsequent reduction in abdominal fat deposition (30). When diet-induced hyperthyroid and hypothyroid chickens were analyzed for their hepatic gene expression, genes involved in the lipogenic pathway experienced the greatest level of differential gene expression between treatment comparisons (19). Also, chickens of the divergently-selected line for leanness experience higher circulating levels of plasma T₃ than chickens divergently-selected for fatness (31).

In a preliminary study (unpublished), the abdominal fat content and free fatty acid levels of four-week-old chickens were dramatically altered after chronic infusion (two weeks) of exogenous corticosterone (CS) or thyroid hormone (T₃), producing a fat and lean phenotype, respectively. T₃ reduced abdominal fat by 40%, whereas CS led to excessive accumulation (61% increase) of abdominal fat as compared with the vehicle control (VC) (Fig. 1.1B). Thus, exogenous corticosterone produced a fat phenotype by stimulating lipogenesis and increasing deposition of body fat. And a lean phenotype was induced by exogenous T₃, which increased metabolic rate and lipolysis.

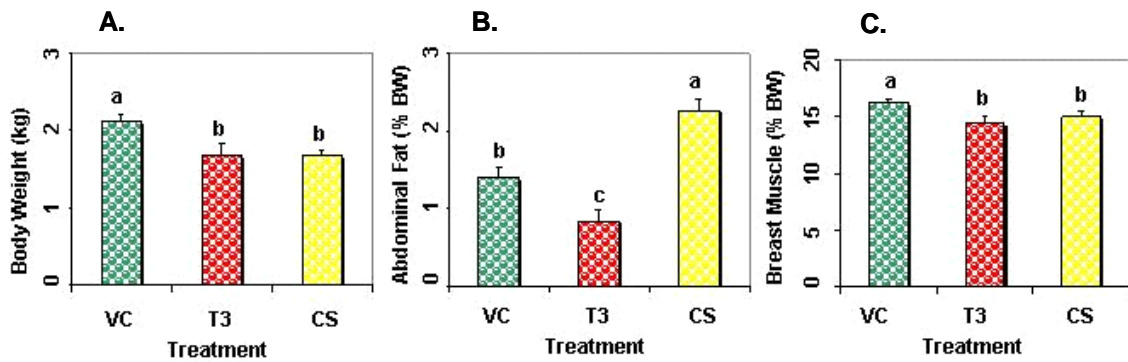


Figure 1.1 Phenotypic response to chronic infusion of hormones (2 weeks). Each value represents the mean of four birds per treatment \pm SEM. Treatments without the same subscript are significantly ($P < 0.05$) different.

This study showed the power of hormonal manipulation to induce obese and non-obese models in an avian system over a 2-week duration. Clearly, the growth and fat accretion of the broiler chicken are regulated by complex interactions between the adrenotropic and thyrotropic axes; however, their exact mechanisms have yet to be defined.

1.3.2 Site of Lipogenesis

It is of interest to mention the difference in anatomical location of lipogenesis in chickens as compared to humans. In birds, lipogenesis (the conversion of glucose to triglycerides), takes place primarily in the liver, whereas the adipocyte serves as the storage site for triglycerides (10). Hepatic lipogenesis plays a direct role in the accumulation of lipid in the avian adipocyte, and 80-85% of the fatty acids stored in adipose tissue are generated through lipogenesis in the liver or from the diet (32). This differs from the mammalian model of fat accretion, where lipogenesis occurs predominantly in the adipose tissue. In spite of these geographic differences in

physiology, mammalian and non-mammalian lipogenesis are likely controlled by the same genes (10). Through analysis of extremes in phenotype (fat versus lean), the genetic contributors to fat accretion and development of obesity can hopefully be elucidated.

1.4 Expectations

Upon alteration of the phenotype in an avian model, transcriptional snapshots of the liver can portray the dynamic genetic profiles responsible for these changes in physiology. Regulation of gene expression in a cell begins at the level of transcription of DNA into messenger RNA (mRNA). Thus, it is of great significance to estimate the relative quantities of mRNA from metabolically-active tissues of lipogenic importance. The experimental perturbations under which a particular gene is up or down-regulated provide vital insight about gene function and metabolic activity, having the potential to reveal the factors that are the cause or effect of the induced pathologic state. Simultaneous expression profiles of many genes can allude to physiological processes or disease etiology that are mediated by the coordinated action of genetic pathways in concert. Upon understanding the genetic and transcriptional control of lipid metabolism at a molecular level, new approaches for clinical therapies can be developed.

The goal of the present study is to build upon the aforementioned hormonal studies on the effect of corticosterone and thyroid hormone in inducing fat and lean phenotypes, respectively, to aid in the understanding of the genetic contribution to obesity and the metabolic syndrome. An acute treatment of exogenous hormones (6 days) will allow investigation of genes responsible for the onset of obesity and its early pathology. As lipogenesis occurs primarily in the liver of birds,

this study will focus on hepatic gene expression. Through the use of newly-developed chicken genomic tools (i.e. microarrays) and bioinformatics, gene networks and metabolic pathways involved in these phenotypic changes will be revealed. This information will be used to identify genes or gene clusters for use in functional mapping of the major metabolic pathways responsible for obesity. Additionally, by observing the combined treatment of CS and T₃, synergistic effects could lead to the discovery of novel gene interactions. These experiments should demonstrate the power of combining hormonal manipulation and microarray analysis to unravel the genetic circuits that control energy metabolism and fat deposition.

Chapter 2

MATERIALS AND METHODS

2.1 Animals and Treatment

Broiler cockerels (Ross x Cobb) were obtained at 1 day of age from a commercial hatchery (Moyer's Hatchery). Only male chicks were used to reduce variability and to simplify experimental design. Chicks were fed a starter ration and raised in a controlled-environment animal room under a 20-h light:4-h darkness photoperiod in a heated battery-brooder until 3 weeks of age. At 3 weeks of age, 72 birds of uniform body weight (± 1 SD) were randomly assigned to wire cages within two identical controlled-temperature rooms with three birds per pen. Rooms were maintained under the same 20L:4D light/dark cycle throughout the duration of the experiment. The pens were divided into four hormonal treatment groups to receive a vehicle (50% DMSO and 50% propylene glycol) as control (VC), exogenous corticosterone (CS), exogenous thyroid hormone (T_3), or both CS and T_3 . Treatment groups were replicated by room. The birds were provided with water and a commercial grower/finisher ration *ad libitum* until the end of the experiment.

At 29 days of age, chickens were given a subcutaneous implant of an osmotic minipump (Alzet® , model 2001; ALZA, Mountain View, CA) to continuously release hormone for seven days at a rate of 1.0 μ l/hour. Corticosterone (CS) and L-tri-iodothyronine (T_3) hormones (Sigma Chemicals, St. Louis, MO) were dissolved in solutions of 50% DMSO and 50% propylene glycol, so as to deliver 600

$\mu\text{g CS/kg/day}$ and $192 \mu\text{g T}_3/\text{kg/day}$, respectively. These dosages were determined based on physiological results from a preliminary study conducted by Dr. Cogburn. Minipumps were filled with hormone solutions the day before implantation and were allowed to incubate in a 0.9% saline solution at 37°C overnight, according to the manufacturer’s protocol. Birds in the combined CS and T_3 treatment group received two minipump implants—one for each hormonal dose—whereas birds from the VC, CS, and T_3 treatment groups received one minipump of their respective dose.

Table 2.1 Experimental design. Number of birds per treatment and age (days) at end of treatment duration are indicated.

TREATMENTS	Age:		
	d30	d33	d36
	<i>Day Post Implantation:</i>		
	1	3	6
VC	6	6	6
T_3 (192 $\mu\text{g/kg/day}$)	6	6	6
CS (600 $\mu\text{g/kg/day}$)	6	6	6
CS+ T_3	6	6	6

Implantation was performed under a sterile surgical procedure to avoid complications from wound infections. The surgical site was removed of feathers and cleaned with a chlorhexidine scrub as described by Ingle-Fehr and Baxter (33). After administration of lidocaine as a local anesthetic, minipumps were inserted subcutaneously through a small incision in the dorsal feather tract of the cervical region. The incision was sealed with wound clips and Vetbond™ Tissue Adhesive (3M Animal Products, St Paul, MN), and the wound was dusted with a Nitrofurazone antibacterial powder (Clay-Park Lab, Bronx, NY) to minimize infection. After implantation, birds were returned to treatment-specific pens and allowed feed and water *ad libitum*. Ambient temperature of each experimental room was monitored

over the duration of treatment, with the mean ambient temperatures being 20.71 °C and 20.47 °C, respectively. Final body weight and feed consumption per pen were recorded at the end of treatment.

On the final day of treatment, a 4 ml blood sample was obtained by cardiac puncture in a Monovette EDTA-treated syringe (Sarstedt, Newton, NC). EDTA treated blood samples were placed on ice and processed immediately. Plasma was obtained by centrifugation, aliquoted to triplicate 1.5 ml microtubes, and stored at -20 °C until assayed. Birds were killed by cervical dislocation on days one (n = 24), three (n = 24), and six (n = 23) days after implantation. Metabolic tissues (liver, breast muscle, and abdominal fat) were excised immediately and snap frozen in liquid nitrogen. Tissues were stored in -80 °C until RNA isolation.

All animals were treated in accordance with the protocols approved by the University of Delaware Animal Care and Use Committee.

2.2 Hormone Assays

Corticosterone. Plasma corticosterone was quantified using an ImmuChem™ Double Antibody Corticosterone I¹²⁵ RIA kit (MP Biomedicals, Orangeburg, NY). Thawed plasma samples were centrifuged for 10 min at 2,000 x g and diluted with steroid diluent. Duplicate aliquots of 100µl of each plasma dilution were added to 12 x 75 mm borosilicate glass, and then assayed according to the manufacturer's protocol. In brief, a CS-specific antibody (rabbit anti-CS) was allowed to bind to ¹²⁵I-labeled CS or plasma-derived CS, with decreased binding of ¹²⁵I-labeled CS corresponding to increased plasma CS levels. Goat anti-rabbit γ-globulin solution was used to precipitate the bound antibody, and radioactivity in the pellet was counted in an Apex Automatic γ-Counter (ICN Micromedic Systems, Huntsville, AL) and the

CS dose (ng/ml) determined from the standard curve. All samples were run in a single assay and detectable in the range of the assay (100-1,000 ng/ml). Intra-assay coefficient of variation for the CS RIA was 25.13% for the low (62-94 ng/ml) and 33.67% for the high (441-661 ng/ml) quality control tubes.

Tri-iodothyronine. A commercial T₃ coated-tube RIA kit (MP Biomedicals) was used to determine plasma T₃ levels. Thawed plasma samples were centrifuged for 10 min at 2,000 x g and diluted with saline. Duplicate aliquots of 100µl of each plasma dilution were added to polypropylene tubes coated with anti-T₃ antibodies (rabbit) (MP Biomedicals). Following the manufacturer's protocol, ¹²⁵I-labeled T₃ was added to each tube before 1-h incubation at 37 °C. Next, tubes were decanted, rinsed with 1 ml of deionized water, and inverted on a rack to dry overnight. Next day, the radioactivity of the tubes was counted in an automatic γ-counter, and the concentration of T₃ (ng/ml) was determined from the standard curve. Samples were run in two different assays and detectable in the range of 0.5 – 8 ng/ml. Intra-assay coefficient of variation (CV) for the combined T₃ RIA assays was 9.03% for the low (1 ng/ml) and 10.6% for the high (4 ng/ml) quality control tubes.

2.3 Plasma Metabolite Assays

Glucose. Plasma glucose levels were measured using an enzymatic colorimetric kit (Sigma Diagnostics, St. Louis, MO). Thawed plasma samples were centrifuged for 10 min at 1000 rpm and diluted in duplicate in polypropylene tubes at 12.5 µl sample to 250 µl water. After the addition of 2.5 ml of a color reagent mixture (Sigma Diagnostics) and incubation at room temperature for 30 min, 200 µl of the reaction mixture was transferred to wells in a 96-well plate. After another 30 min incubation period at room temperature, the plate was read at 450 nm in a SpectraMax

190 microtiter plate reader (Molecular Devices, Sunnyvale, CA). The absorbance of a serially-diluted standard was used to calculate glucose concentrations of each plasma sample. All samples were detectable in the range of the assay (50 – 400 mg/dl).

Triglycerides. The quantity of triglyceride in plasma was determined using a L-type Triglyceride H assay kit (Wako Chemicals, Richmond, VA), according to the manufacturer's instructions. Thawed plasma samples were centrifuged for 10 min at 1000 rpm and then 5 µl of each sample was added to respective wells in a 96-well microtiter plate. 80 µl of Enzyme Color A (Wako) was added to each well and allowed to incubate for 5 min at 37 °C, followed by a reading of the sample absorbencies at 600 nm/700 nm in a SpectraMax 190 (Molecular Devices). After 40 µl of Enzyme Color B (Wako) was added and allowed to incubate for another 5 min at 37 °C, the absorbencies of the samples were again measured in the microtiter spectrophotometer. Sample absorbencies were compared to a standard curve to determine triglyceride concentration. Samples were run in three different assays and detectable in the range of 55 – 392.8 mg/dl.

Non-esterified fatty acids (NEFA). Plasma NEFA concentrations were determined using a NEFA-C assay kit (Wako), according to the manufacturer's instructions. Thawed plasma samples were centrifuged for 10 min at 1000 rpm and then 10 µl of each sample was added to respective wells in a 96-well microtiter plate. Next, 50 µl of Color Reagent A (Wako) was added to each well and allowed to incubate for 10 min at 37 °C. Following incubation, 150 µl of Color Reagent B (Wako) was added to each well and allowed a second incubation for 10 min at 37 °C. The plate was then read at 550 nm in a SpectraMax 190 (Molecular Devices). Sample absorbencies were compared to a standard curve to determine NEFA concentration.

Samples were run in two different assays and detectable in the range of 0.25 – 2 mEq/l.

2.4 Total RNA Isolation from the Liver of Day 6 Birds

Total RNA from liver samples of birds that received six days of treatment was isolated using a RNeasy Midi kit (Qiagen, Valencia, CA) following the manufacturer's protocol with some modifications. Frozen hepatic tissue samples (~0.20 g) were homogenized in a buffer containing β -mercaptoethanol using a Polytron 3000. The resulting cell lysate was centrifuged for 10 min at 3,300 x g and 20 °C. This procedure was modified for samples with low initial RNA yield, due to high fat content in homogenate, by adjusting the centrifugation to 20 min at 4 °C. The supernatant was transferred to new tubes and mixed with equal volumes of 70% ethanol, which was then loaded in aliquots onto a midi spin column and centrifuged for 15-20 min at 3,300 x g and 20 °C. After centrifugation, any remaining liquid in the spin column was removed by pipet. Next, the samples were purified through three wash spins using the buffers provided by the Qiagen RNeasy Midi kit. At 3,300 x g and 20°C, the first wash was centrifuged for 5 min, the second wash was centrifuged for 2 min, and the third wash was centrifuged for 10 min. RNA was then collected through two elutions of the midi spin column after allowing 1 min of incubation before each elution. At 3,300 x g and 20°C, the first elution was performed with 200 μ l RNase-free water and centrifuged for 3 min, and the second elution was performed with 150 μ l RNase-free water and centrifuged for 15 min. The resulting elutant was mixed with 1/10 volume of sodium acetate and 2 volumes of 95-100% ethanol (-20 °C) and placed in -80 °C overnight to precipitate. After centrifugation for 30 min at 15,000 rpm and 4 °C, the pellet was washed twice with 500 μ l of 70% ethanol and

centrifuged for 5 min at 15,000 rpm and 4 °C to remove impurities. The washed RNA pellet was then dried in a vacufuge for 20 min at 45 °C and reconstituted in RNase-free water. The quantity of extracted total RNA was determined using a NanoDrop spectrophotometer (Wilmington, DE), and the quality of extracted total RNA was examined by microcapillary electrophoresis on a BioAnalyzer 2100 (Agilent, Wilmington, DE), where the rRNA ratio (28S/18S) was observed for integrity. When not in use, total RNA samples were stored in –80°C.

2.5 Microarrays

Del-Mar 14K Chicken Integrated Systems Microarrays (Geo Platform # GPL1731), as described previously (10), were used for the identification of differential gene expression from the 23 birds that received six days of treatment. Chicken cDNA targets were synthesized through an indirect cDNA dye labeling method, in order to minimize dye bias caused by direct incorporation of dye into the cDNA strand during the reverse transcriptase reaction (34;35). First, total RNA samples (20 µg) were reverse transcribed using an anchored Oligo(dT)₂₀ Primer, amino-modified dNTPs, and Superscript™ III Reverse Transcriptase (Invitrogen) in 30 µl volume. Next, the RNA template was destroyed by incubation with sodium hydroxide at 70 °C. First strand cDNA was purified with a Low-Elution Volume Spin Cartridge (Invitrogen) and then labeled with Alexa Fluor® 555 (green) or Alexa Fluor® 647 (red) (Invitrogen) in a fluorosecent dye coupling reaction. Dye-incorporated cDNAs were purified to remove un-reacted dye and analyzed for their labeling efficiency with a NanoDrop spectrophotometer. The targets were then resuspended in 30 µl DIG Easy Hyb Solution (Roche) supplemented with 25 µg salmon testes DNA (Sigma), 25 µg yeast tRNA (Sigma), and 2.5 µl of PCR-amplified

pSport 6.1 vector. After pre-hybridization of the microarray slides in blocking reagent (1% BSA, 5 × SSC, 0.2% SDS) bubbled with nitrogen gas, each slide was hybridized with a sample labeled with Alexa Fluor® 555 (green) and a pooled reference sample labeled with Alexa Fluor® 647 (red) in a reference hybridization design. A reference sample was made from equal amounts of RNA pooled from each of the six birds that received vehicle control for six days. The slides used for hybridization came from a single batch printed by the Delaware Biotechnology Institute Microarray Core on June 3rd, 2004. Heat denatured targets were then applied to array slides under a 22 x 65 mm glass coverslip (LifterSlip cover glass, Erie Scientific) in individual hybridization chambers. Slides were hybridized overnight in a 42 °C water bath under a light-tight box. On the following day, slides were washed with 1×SSC, 0.2% SDS, and 0.5% DTT at 55 °C for 10 min, then 0.1 × SSC, 0.2% SDS, and 0.5% DTT for 5 min at room temperature, and finally 0.1 × SSC and 0.5% DTT for 1 min at room temperature, with N₂ gas bubbled through each of the washes to prevent interference of ozone. The slides were subsequently rinsed in dH₂O and dried by centrifugation. Before scanning, slides were stored in individual 50 ml tubes covered in aluminum foil and filled with N₂ gas.

2.6 Image Acquisition and Analysis

Slides were scanned using an Axon 4100A Microarray Scanner (Axon Instruments) with GenePix Pro 5.0 software (Axon Instruments) and at a PMT count ratio (635/532) of about 1. Spots were manually checked for quality and eliminated for inadequacies in signal, heterogeneity, background, and/or morphology. The results of image analysis were automatically merged with Excel files containing the clone identification number/plate address and gene name/function (from the highest

BLAST score). For statistical analysis, \log_2 -transformed fluorescence intensities were analyzed with a two-step mixed model analysis of variance (ANOVA) using SAS software (36;37). The first step normalized for variability that was array-specific, and the second step used gene-specific models to test the effect of treatment on expression profiles for individual genes. To adjust for the inherent testing problem of multiple comparisons between the thousands of genes on the array, an adjustment made with Bonferonni's method assured an experimentwise false discovery rate (FDR) of 0.05 (36). Genes were considered differentially expressed if FDR was $P < 0.05$. In order to avoid the elimination of biologically relevant genes, simple fold-change cut-off values were not imposed, because genes with small fold-changes have the potential to cause cascade events that significantly alter lipid metabolism (36). Thus, each gene was assessed uniquely based on statistical significance in variability instead of enforcing global cut-off values. The values of fold changes were based on the adjusted ratio between treatment comparisons. The differentially expressed genes from the microarrays were clustered according to similarities in gene expression patterns with the aid of GeneSpring GX 7.3 software (Agilent). Subsequent Pathway Miner analysis (38) used \log_2 transformation of the adjusted ratio CS/T₃ values. EST clones that represent high-scoring contigs were subjected to BlastX analysis to identify chicken orthologs of human proteins. However, GO annotation was only achieved for roughly half of the differentially expressed non-redundant genes (1,102 genes). Furthermore, GO annotation was mainly accomplished for the cDNA probes that represent high scoring contigs. The human protein tagged chicken cDNA probes were used along with the \log_2 of the fold differences between treatment conditions. In addition, significant differentially expressed genes were annotated with gene ontology

(GO) terms and clustered into three GO-categories (molecular function, cellular component, and biological process) using the GOSlimViewer tool feature at the AgBase site (<http://www.agbase.msstate.edu/>).

2.7 Real-time Reverse Transcription-Polymerase Chain Reaction Quantification of mRNAs

Two-step real-time quantitative RT-PCR was used to verify gene expression patterns of 5 genes that were identified as differentially expressed through the microarray screening. An additional 12 genes not found to be differentially expressed on the microarrays were also analyzed with real-time qRT-PCR because of their known involvement in lipid metabolism (32;39;40). Primers were designed with Primer Express Software (Applied Biosystems, Foster City, CA) from the contig or singlet sequence (14) and synthesized by Sigma-Genesis (The Woodlands, TX). The sequences for forward and reverse primers used for the amplifications are shown in Table 2.2. The specificity and efficiency of the primers were validated by agarose gel electrophoresis and confirmed to give a single amplified band of appropriate size.

DNase Digestion. To eliminate genomic DNA contamination before subsequent RT-PCR, total RNA samples were treated with RNase-free DNase. Following a Qiagen RNeasy Mini protocol with slight modification, 5 μ l of DNase I was added to samples and allowed to incubate for 30 min at room temperature. Next, 350 μ l Buffer RLT (Qiagen) was added to the sample, followed by the addition of 250 ml ethanol. The sample was then applied onto a mini spin column and centrifuged for 15 s at 8,000 x g and 20 °C. After centrifugation, the samples were purified through two wash spins using the buffers provided by the Qiagen RNeasy Mini kit. The washes were centrifuged at 8,000 x g and 20 °C for 15 s and 2 min, respectively.

After a final centrifugation for 1 min at 14,000 x g and 20 °C, the sample was collected through two elutions of the mini spin column with RNase free water for 1 min at 8,000 x g and 20 °C. The quantity of cleaned total RNA was measured using a NanoDrop spectrophotometer, and the quality of cleaned total RNA was assessed by examining the 28S and 18S transcripts on an ethidium bromide-stained 1.2% formaldehyde agarose gel. To confirm that genomic DNA contamination was eliminated, cleaned total RNA samples were compared to DNA, cDNA, and water controls through PCR with PK primers. After addition of 1.5 µl 10X buffer, 0.5 µl dNTP mix, 0.5 µl PK primer forward, 0.5 µl PK primer reverse, 0.1 µl Taq polymerase, and RNase-free water to total 14 µl, the PCR was performed at 94 °C for 5 min, 32 cycles of 94 °C for 15 s, 60 °C for 30 s, and 72 °C for 1 min, and 72 °C for 5 min. PCR was performed in a 96-well plate using Thermal Cycler. The PCR products were electrophoresed on an ethidium bromide-stained 2% agarose gel and visualized in a gel document station (Alpha Innotech Corp., San Leandro, CA).

Reverse Transcriptase Reaction. DNase-cleaned total RNA was reverse transcribed to cDNA by first adding 2.5 µl cleaned total RNA, 1 µl anchored Oligo dT primer (Invitrogen #55117 2.5 µg/µl), 1 µl 10 mM dNTPs, and RNase-free water to 13 µl to a 96-well plate and heating for 5 min at 65 °C. After incubating the mixture on ice for 2 min, 4 µl 5X first strand buffer, 1 µl 0.1 M DTT, 1 ml RNase Out (40 U/µl), and 1 µl SuperScript III RT were added to each sample. The mixture was incubated at 46 °C for 2 hours in a Gene Amp® PCR System 9700 Thermal Cycler (Applied BioSystems) and then heated at 70 °C for 15 min to inactivate the reaction. After diluting the resultant cDNA template 1:5 with RNase-free water, the samples were

transferred to 1.5 ml microcentrifuge tubes and stored in -20 °C until amplification with appropriate primers.

Real-time quantitative PCR. qPCR was performed in 384-well plates in 10 or 20 μ l reaction volumes containing 1 μ l of diluted (25 ng/ μ l) cDNA, a 10 μ M concentration of the forward and reverse primers, 2X SYBR Green PCR Master Mix (Qiagen), and DNase-free water. Each sample was assayed in duplicate for each gene, and the reactions were performed with a PRISM® 7900HT Sequence Detection System (ABI; Fullerton, CA). Serially diluted plasmid samples of known quantity were amplified with APOC3 primers and used as a standard curve per plate to allow absolute quantification. The amplification protocol included an initial denaturing step at 95 °C for 15 min followed by 40 cycles of a 95 °C denaturing step for 15 s and a 60 °C annealing step for 1 min. Following amplification, a dissociation step was performed at 95 °C for 15 s, 60 °C for 15 s, and then 95 °C for 15 s. After analyzing the dissociation curve for accuracy in amplification, relative gene expression values were quantified using a version of the ΔC_T method as described by Livak and Schmittgen. The data were transformed using the equation $2^{-\Delta C_t}$, where C_t represents the fractional cycle number when the amount of amplified PCR product reached an arbitrary threshold value (0.72 for all plates) within the exponential growth region of the amplification curve, and ΔC_t is the difference between the sample C_t and the highest C_t for each gene, respectively. The qRT-PCR data are presented as gene expression in arbitrary units (AU).

Table 2.2 Primers used for real-time qRT-PCR.

Gene ¹ Name	GenBank Number	Primer Sequence (5'-3')	Orientation	Amplicon (bp)
<i>ACACA</i>	NM_205505	AGGAGGGAAGGGAATTAGGAAA GATCGGAGAGCCTGGGACTT	Forward Reverse	91
<i>ADRP</i>	BM427568	GGAGAGCAAACAGCTTGAACACA CCAAGGCTTTTGACAGCTACA	Forward Reverse	111
<i>AFABP</i>	BM425789	CAGAAGTGGGATGGCAAAGAG TGCATTCCACCAGCAGGTT	Forward Reverse	70
<i>APOB</i>	BG641848	CTTGGGCCATAGGGCTTACTC TGATCCAACAAACATGGAAAACA	Forward Reverse	78
<i>APOC3</i>	UD_Contig_15342.468	CACGGCCATCCTGGC CAGCTTCCAGAGCTCG	Forward Reverse	305
<i>DEFB9</i>	AY621324	GTGGTGGGAAGCTGAAATGC TGATGTCATAAGGCAGGAGACATC	Forward Reverse	114
<i>FAS</i>	BG711257	ACTGTGGGCTCCAAATCTTCA ACCGGTGTTGGTTTGCAA	Forward Reverse	96
<i>Fath</i>	BM489839	GAGTCAATACAGCCTCCCAGAGA AACCTCTGCCTGCTTCTGTAGA	Forward Reverse	74
<i>LDHB</i>	BM425573	ACAGCGAGAACTGGAAGGAA AGCTCAGCAACGCTAAGACC	Forward Reverse	109
<i>LPL</i>	AW355477	TGCTGGTCCCACCTTTGAGTA TGCAGGACATCCACAAAGTCA	Forward Reverse	78
<i>ME1</i>	NM_204303	TGGACAGGGTAACAATTCCTACGT CAGGCGACCTTCCTGTAAATTC	Forward Reverse	105
<i>PEPCKC</i>	BM440800	CATGACACGGATGGGAACAG GAGTGAAGGCATTTCAAAATTCTC	Forward Reverse	69
<i>PEPCKM</i>	NM_205470	GCCCCTTTTCGGCTACAAC TTCGTTATCTCGGAGGAACCA	Forward Reverse	119
<i>PK</i>	BI066928	CTGAAATCCGAACTGGACTCATC GAGAGCTGCGCCCTTCTTG	Forward Reverse	71
<i>SCD1</i>	BG711877	CACCGTGTCCACCACAAGTTC AGAAGCCCCGCATAGCATT	Forward Reverse	64
<i>SOD3</i>	BI391278	CCAGTGATGGCTGATAATGAGACT CTATTTTGAGCTGGGCTTCA	Forward Reverse	73
<i>THRSP</i>	AY568629	TTCTCGGCCACGCAGAAG AAGACCCCTCGCAGCAGG	Forward Reverse	71

¹*ACACA*: Acetyl-Coenzyme A carboxylase alpha; *ADRP*: Adipose differentiation-related protein (adipophilin); *AFABP*: Fatty acid-binding protein, adipocyte; *APOB*: apolipoprotein B; *APOC3*: Apolipoprotein C-III; *DEFB9*: β -defensin 9 (Gallinacin 6); *FAS*: Fatty acid synthase; *Fath*: Fat 1 cadherin; *LDHB*: Lactate dehydrogenase B; *LPL*: Lipoprotein lipase; *ME1*: Malic enzyme 1; *PEPCKC*: Phosphoenolpyruvate carboxykinase, cytosolic; *PEPCKM*: Phosphoenolpyruvate carboxykinase, mitochondrial; *PK*: Pyruvate kinase; *SCD1*: Stearoyl-CoA desaturase (delta-9-desaturase); *SOD3*: Superoxide dismutase 3; *THRSP*: thyroid hormone responsive protein Spot 14

2.8 Statistical Analyses

This experiment had a factorial design (4×3) with four different treatment groups and three different days (1, 3, and 6 days post-implantation) for collection of tissues samples. Chickens were assigned to cages according to a randomized-complete-block design with pen and environmental room as replicates. Data for final body weight, total feed intake, hormone assays, plasma metabolite assays, and real-time qRT-PCR were analyzed as a completely randomized design using PROC GLM of the Statistical Analysis System (SAS Institute, Inc., Cary, NC). Pairwise comparisons of treatment were tested for significance with a Fischer's least significance difference t test ($P < 0.05$). The statistical model also included random effects of time (day of treatment), hormone treatment, and experimental room, as well as all two and three-way interactions (time×treatment, treatment×room, time×room, and time×treatment×room). Data are expressed as the mean and the standard error of the mean (\pm SEM).

Chapter 3

RESULTS

3.1 Inducing Obesity, the Phenotypic Response to Exogenous Hormones

Hormonal treatment with osmotic minipumps resulted in the elevation of CS or T₃ in birds of the respective treatment. Birds receiving treatment of exogenous CS, alone, showed elevated ($P < 0.05$) levels of plasma CS in the Day 1 (3-fold) and Day 6 (5-fold) treatment groups (Fig. 3.1A). The CS-treated birds in the Day 3 treatment group did not have significantly higher levels of CS compared to the vehicle control birds, but showed higher ($P < 0.05$) levels of CS than that of the T₃ birds. With the exception of the Day 1 birds, birds of the CS+T₃ treatment did not exhibit significantly higher levels of plasma CS compared to respective control birds. However, the Day 6 birds of the CS+T₃ treatment showed higher ($P < 0.05$) levels of plasma CS than birds of the respective T₃ treatment group. No significant differences in plasma CS were found between control birds and birds receiving exogenous T₃ (Fig. 3.1A). Thus, as early as 24 hours after implantation, CS treated birds exhibited an elevated-corticosterone state.

The average plasma T₃ levels were elevated ($P < 0.05$) by T₃, alone (5.6-fold) or in combination with CS (3.5-fold), across the three days of treatment (1, 3, and 6 days) (Fig. 3.1B). No significant differences in plasma T₃ were found between T₃ and CS+T₃ treated birds of the 3 and 6-day treatment duration. Also, no significant differences in plasma T₃ were found between control birds and birds receiving

exogenous CS (Fig. 3.1B). Thus, each bird receiving treatment of exogenous T₃, alone or in combination with CS, had been rendered hyperthyroid, whereas the birds not receiving exogenous T₃ remained euthyroid.

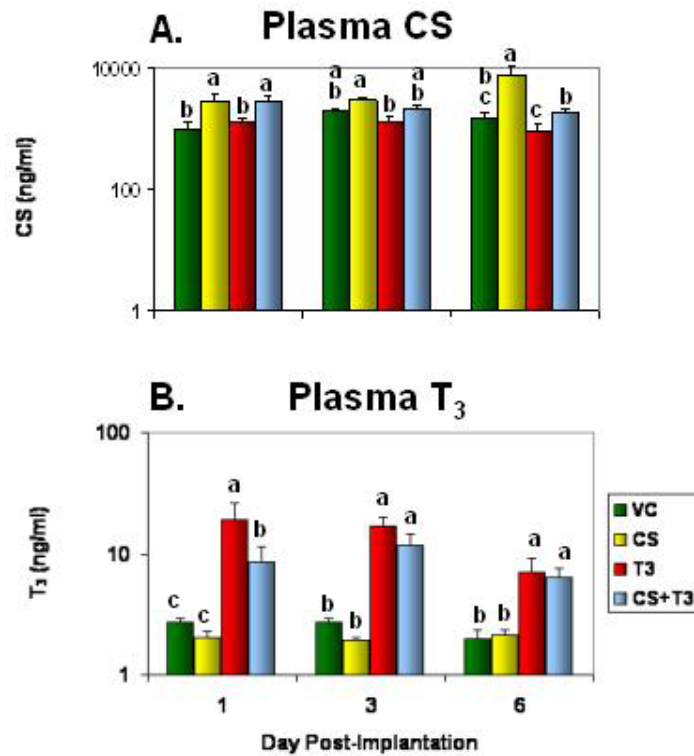


Figure 3.1 Elevation of circulating hormone levels with infusion of exogenous hormones. Plasma levels of corticosterone (CS) (A.) and plasma levels of tri-iodothyronine (T₃) (B.) are shown on a logarithmic scale. Control birds (VC) are represented as green, CS as yellow, T₃ as red, and CS+T₃ as blue. ‘Day Post-Implantation’ indicates duration of hormonal treatment (1, 3, or 6 days). Each value represents the mean ± SEM of six birds per treatment, except for CS+T₃ Day 6, which is the mean ± SEM of five birds. Treatments without the same superscript are significantly ($P < 0.05$) different.

Body weight and total feed intake at end of treatment were useful indicators of phenotypic changes. Although final body weights were slightly depressed by either exogenous treatment with CS or T₃ compared to controls, they were not significantly different (with the exception of Day 3 T₃ birds) (Fig. 3.2A). However, birds receiving both minipumps for CS and T₃ did show lower ($P < 0.05$) final body weights (Fig. 3.2A). In comparison to other respective treatments, total food intake over the duration of treatment was higher ($P < 0.05$) in the CS treated birds and lower ($P < 0.05$) in the CS+T₃ treated birds (Fig. 3.2B). In other words, the CS birds were eating more yet weighing the same as control birds, whereas the CS+T₃ birds were eating less and, correspondingly, weighing less than all other birds.

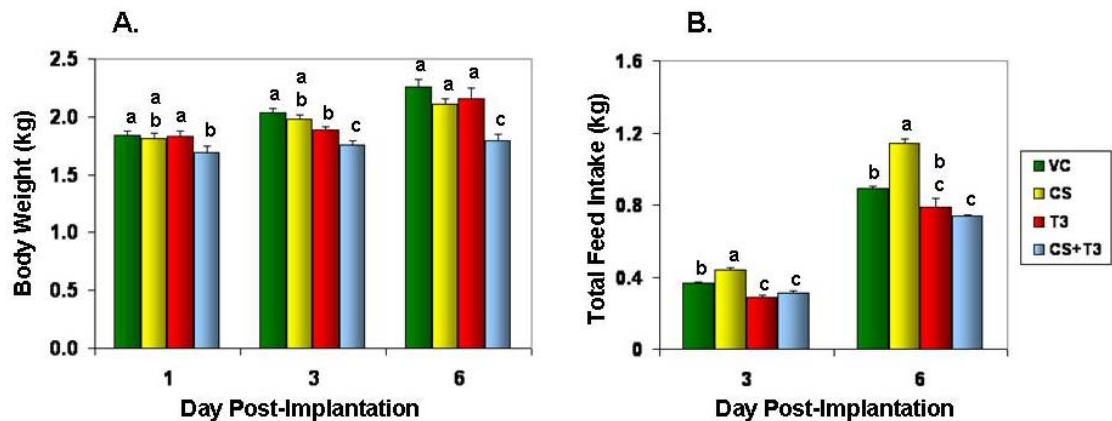


Figure 3.2 Final body weight (A.) and total feed intake (B.) of chickens after acute hormonal treatment. VC is represented as green, CS as yellow, T₃ as red, and CS+T₃ as blue. ‘Day Post-Implantation’ indicates duration of hormonal treatment (1, 3, or 6 days). Each value represents the mean \pm SEM of six birds per treatment, except for CS+T₃ Day 6, which is the mean \pm SEM of five birds. Treatments without the same superscript are significantly ($P < 0.05$) different.

Plasma metabolite levels were another indicator of the physiological response to exogenous hormones. Birds from the CS treatment group maintained higher ($P < 0.05$) plasma glucose levels at Days 1 (1.6-fold), 3 (1.2-fold), and 6 (1.4-fold) compared to control birds (Fig. 3.3A). Plasma triglyceride levels were also elevated ($P < 0.05$) in CS birds compared to all other treatments and increased slightly from days 1 to 6 after implantation, reaching the highest level on day 6 (3.9-fold) (Fig. 3.3B). This paralleled a similar increase in plasma levels of non-esterified fatty acid (NEFA) seen in the CS birds (Fig. 3.3C). Furthermore, NEFA levels were higher ($P < 0.05$) for birds receiving CS treatment, alone or in combination with T_3 , compared to control birds on days 3 (1.4-fold and 1.3-fold, respectively) and 6 (1.5-fold and 1.4-fold, respectively) after implantation (Fig. 3.3C). The plasma glucose and triglyceride levels of CS+ T_3 treated birds remained relatively constant throughout the duration of treatment and exhibited no significant differences compared to control birds (Fig. 3.3A and B). All three metabolite indicators (glucose, triglycerides, and NEFA) remained relatively constant for the T_3 -treated birds, and, except for the triglyceride level on Day 3, were not significantly different from control birds (Fig. 3.3). Consequently, after 6 days of treatment, drastic changes in plasma metabolite levels were observed by comparison of treatments, with the CS treated birds having consistently higher levels of plasma glucose, triglyceride, and NEFA.

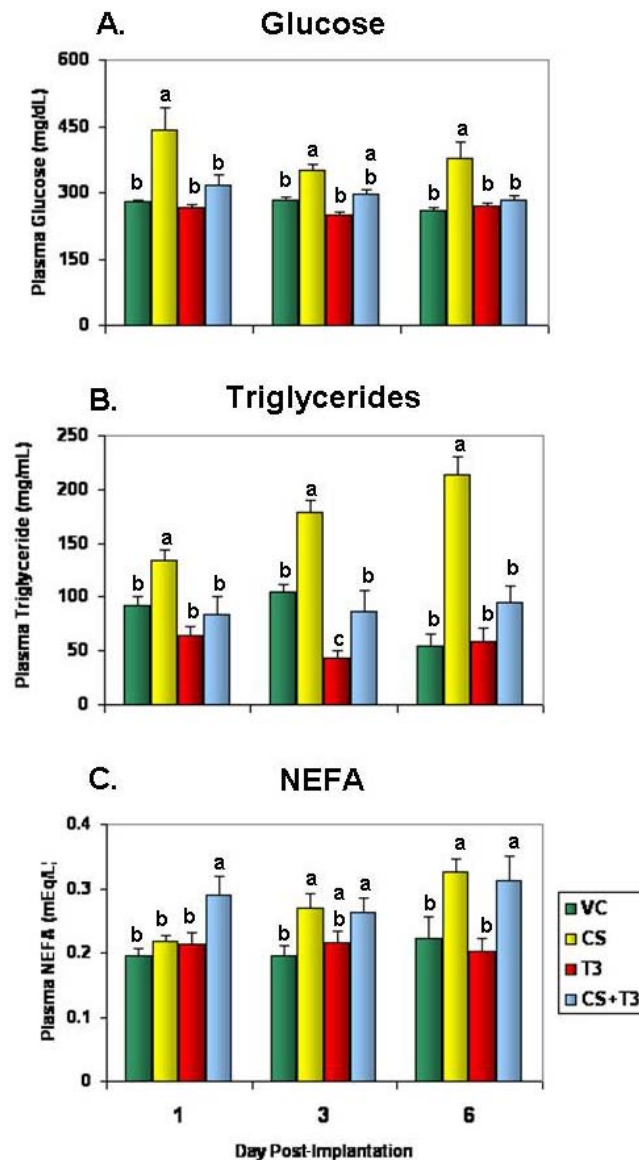


Figure 3.3 Plasma metabolite response to infusion of exogenous hormones. Plasma glucose (A.), plasma triglycerides (B.), and plasma non-esterified fatty acids (NEFA) (C.) are shown. Birds treated with VC are represented as green, CS as yellow, T₃ as red, and CS+T₃ as blue. ‘Day Post-Implantation’ indicates duration of hormonal treatment (1, 3, or 6 days). Each value represents the mean ± SEM of six birds per treatment, except for CS+T₃ day 6, which is the mean ± SEM of five birds. Treatments without the same superscript are significantly ($P < 0.05$) different.

3.2 Microarray Analysis and Identification of Differentially Expressed Genes

Analysis of gene expression data from 23 microarrays represents changes in hepatic gene expression in birds at 6 days of treatment (6 birds per treatment, except for 5 birds from CS+T₃). A total of 1,824 transcripts were found differentially expressed across the four treatment groups. The detailed gene lists can be found on the project website (<http://cogburn.dbi.udel.edu/>) under the Gene Expression button. Differential expression is based on a false discovery rate (FDR) ($P < 0.05$), which is an arbitrary cut-off level that indicates the highest probability of being truly differentially expressed between treatment groups. Because some genes were represented by multiple cDNA probes on the array, the 1,824 differentially expressed transcripts actually correspond to 1,102 non-redundant gene transcripts after duplicate contigs were deleted. Table 3.1 shows the number of genes that were differentially expressed (induced or suppressed) by treatment comparison. The greatest number of differentially expressed genes were between the CS and T₃ comparison (763 genes), whereby the majority (70%) of the genes in this comparison were down-regulated by CS (or up-regulated by T₃). In fact, all treatment comparisons with CS revealed greater numbers of differentially expressed genes than contrasts made with T₃ or CS+T₃. Also, CS infusion increased the number of down-regulated genes when compared to other treatments. In addition, the T₃ versus VC contrast revealed the fewest number of differentially expressed genes (14 genes).

Furthermore, Fig. 3.4 shows that no differentially expressed genes were common to all three treatment comparisons versus the control. Only 4 differentially expressed genes were common to CS and CS+T₃ compared to controls, and 1 differentially expressed gene was in common to T₃ and CS+T₃ compared to controls

(Fig. 3.4). Thus, when compared to the control, the majority of differentially expressed genes were specific to treatment.

Table 3.1 Differentially expressed hepatic genes by treatment contrast. Values represent non-redundant differentially expressed genes with false discovery rates (FDR) $P < 0.05$, as determined by two-step mixed model ANOVA of microarrays.

Comparisons	Up-regulated	Down-regulated
CS vs. VC	157	306
T ₃ vs. VC	8	6
CS+T ₃ vs. VC	33	3
CS vs. T ₃	231	532
CS vs. CS+T ₃	123	320
T ₃ vs. CS+T ₃	11	25

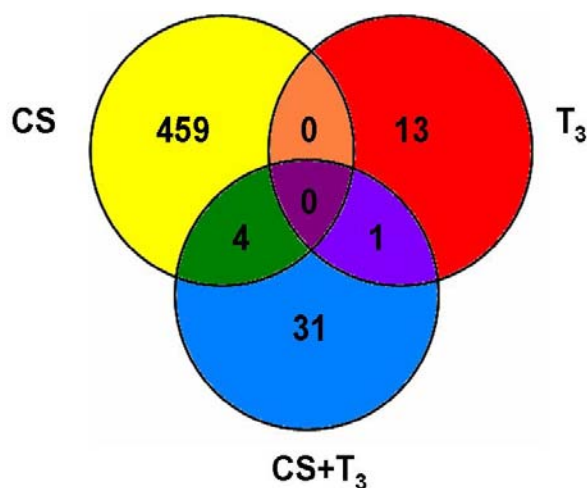


Figure 3.4 Venn diagram showing three major gene clusters that were either up- or down-regulated with CS, T₃, or CS+T₃ treatment as compared to vehicle control, respectively. Common genes shared between treatment contrasts are presented in the overlapping areas.

Upon analysis of the microarrays with GeneSpring GX 7.3 software (Agilent), expression patterns were revealed by hierarchical clustering of treatment groups (Fig. 3.5). The CS cluster shows down-regulation of genes represented in the upper part of the column, as indicated by the blue saturated boxes, and up-regulation of genes represented in the lower part of the column, as indicated by the red saturated boxes. The T₃ cluster shows an opposite pattern with less dramatic up-regulation (less saturated red boxes) in the upper portion of the T₃ column and less prominent down-regulation in the lower portion of the T₃ column (less saturated blue boxes). The CS+T₃ cluster indicated a dampened response similar to CS treatment, alone, as indicated by the less saturated blue boxes in the upper part of the column. However, CS+T₃ also appears to have similar expression patterns as T₃, alone, on a number of genes. As would be expected, the VC cluster contains predominantly genes with no fold-difference (yellow hue), because the dual fluorescence array hybridized each VC bird against a reference pool of all vehicle control birds, so only minor differential expression due to deviations from the mean expression level of the VC treatment would be observed.

All microarrays from CS and CS+T₃ birds clustered with their respective treatment group. The specific clustering pattern observed from the dendrogram revealed that the CS+T₃ treated birds had gene expression patterns that were more similar to those of the CS treated birds than to those of the T₃ or control birds. Interestingly, not all of the microarrays from T₃ treated birds clustered into a unique cluster. The T₃ microarrays revealed expression patterns that were actually more similar to the control microarrays, with one of the T₃ slides even having a closer

similarity to the control than to slides from other T₃ birds. Also, most peculiar, one of the T₃ slides clustered highly similar to expression with the CS treatment cluster.

3.3 Functional Classification of Differentially Expressed Genes

The exhaustive list of differentially expressed genes indicated through microarray analysis was compared to human protein databases to retrieve gene ontology (cellular component, biological process, and molecular function) annotations for these chicken orthologues. Of the 1,824 differentially expressed transcripts, only a fraction (about 50%) identified with their homologous human protein and contributed to the graphical representation in Fig. 3.6. The cellular component was recognized for 492 genes and divided into 12 categories (Fig. 3.6A); the biological process was recognized for 635 genes and divided into 19 categories (Fig. 3.6B), and the molecular function was recognized for 813 genes and divided into 26 categories (Fig. 3.6C). Concerning cellular compartment, the majority of genes coded for proteins in the cytoplasm and membrane (38.1% and 25.6%, respectively) (Fig. 3.6A). The three most represented categories of biological process were metabolism, transport, and nucleic acid metabolism (14.8%, 14.5%, and 13.9%, respectively) (Fig. 3.6B). When looking at molecular function, the largest percentage of genes was involved in binding (26.1%) (Fig. 3.6C).

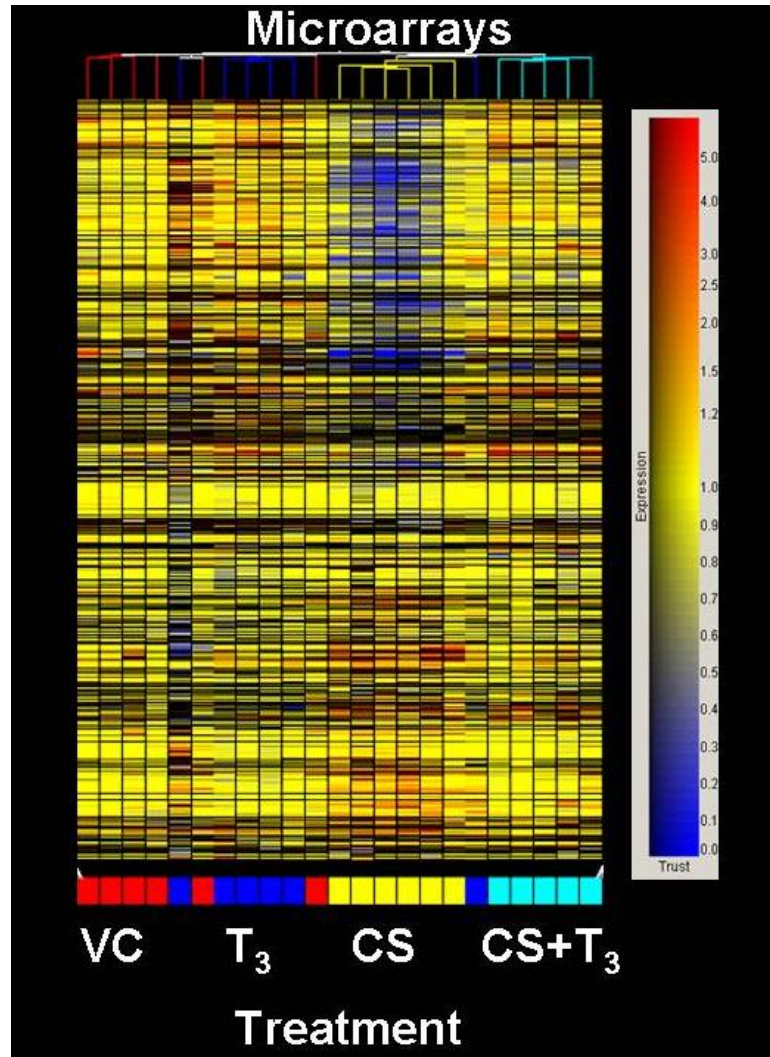
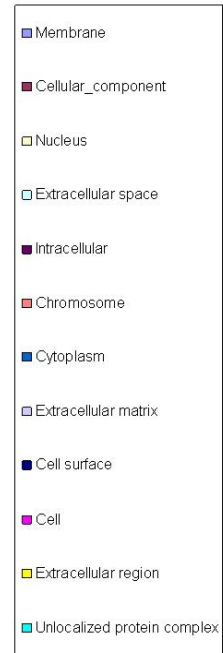
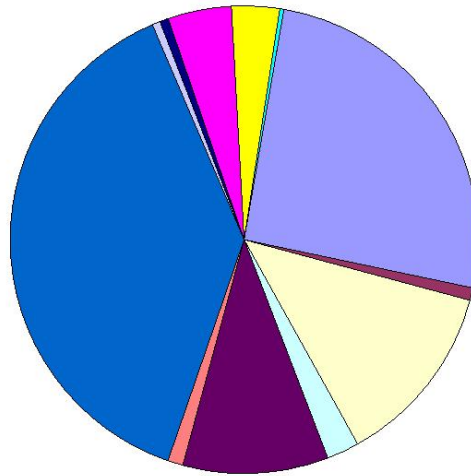


Figure 3.5 Hierarchical Clustering (GeneSpring) of genes (Y-axis), treatments (VC, CS, T₃, or CS+T₃) and their biological replications (X-axis). Each gene contig is represented by a single row of colored boxes; each bird (microarray) is represented by a single column. Gene expression profiles are indicated in a saturated color scale with up-regulated genes (red) and down-regulated genes (blue). Birds treated with VC are represented by red branches, T₃ with blue branches, CS with yellow branches, and CS+T₃ with light blue branches.

A. Cellular Component



B. Biological Process

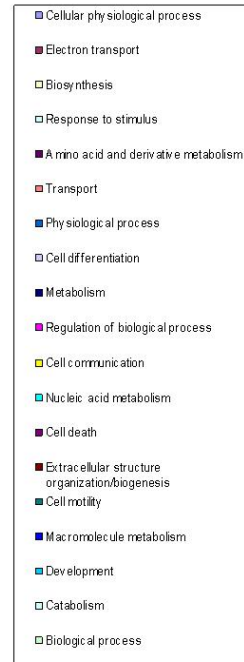
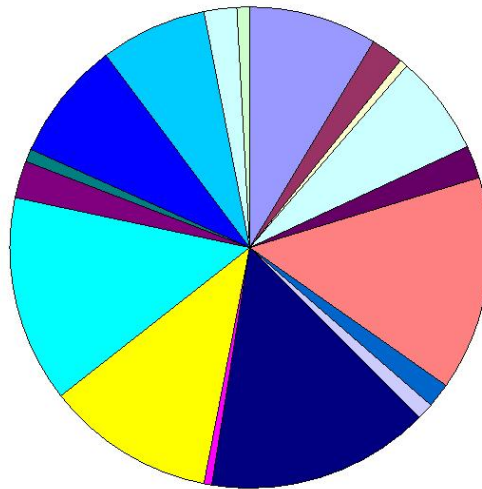


Figure 3.6 *(Legend appears on next page.)*

C.

Molecular Function

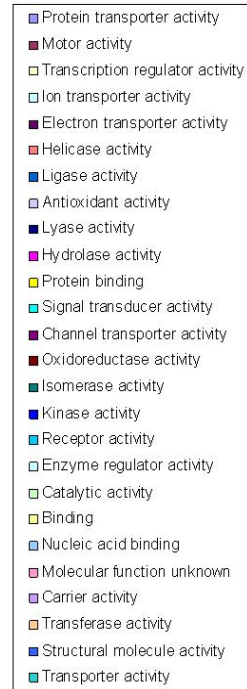
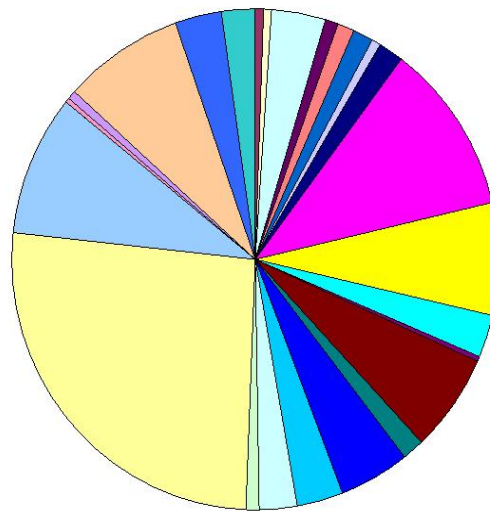


Figure 3.6 (Continued from previous page) **Pie Charts of the three major gene ontology (GO) categories of differentially expressed hepatic genes.** From a total of 1,102 non-redundant differentially expressed genes, the (A.) cellular component of 492 genes, (B.) biological process of 635 genes, and (C.) molecular function of 813 genes were identified with BlastX against protein databases for annotation with GO terms. The data were generated by submission of the differentially expressed gene list into the GOSlim tool on the AgBase website (<http://www.agbase.msstate.edu/>).

Pathway Miner analysis of the differentially expressed genes between the CS and T₃ comparison provided additional insight into gene function and affiliated pathways. However, the pathway analysis only included 231 genes out of the 763 differentially expressed between CS and T₃; thus, not all pathways containing the full list of perturbed genes are represented. Table 3.2 notes a few of the key cellular and regulatory pathways. Most interesting to note are those pathways involved in transcriptional regulation (MAPK and Wnt signaling pathways) and the pathways involved in the inflammatory response (Inflammatory Response Pathway, IL-10 Anti-inflammatory Signaling Pathway, and Complement Activation). Both transcriptional regulation pathways contain genes that are up and down-regulated by CS and T₃. The inflammatory response pathway contains only those genes that are down-regulated by CS (up-regulated by T₃). Fig. 3.7 shows genes that are associated in a number of interconnecting cellular and regulatory pathways.

Table 3.3 notes some of the more important metabolic pathways represented by the differentially expressed genes of the CS versus T₃ contrast. The majority of the genes involved in these pathways (Glycolysis/Gluconeogenesis, ATP synthesis, Fatty acid metabolism) are down-regulated by CS (or up-regulated by T₃). However, there are two exceptions. In glycolysis/gluconeogenesis, phosphofructokinase-liver (*PFKL*) and dihydrolipoamide dehydrogenase (*DLD*) are up-regulated by CS (down-regulated by T₃), and in fatty acid metabolism, acetyl-Coenzyme A acetyltransferase 2 (*ACAT2*) is up-regulated by CS (down-regulated by T₃) (Table 3.3). Fig. 3.8 shows how these genes interconnect in a number of metabolic pathways. Of interest is the cluster of *ACAT2*, *EHHADH*, *HADH2*, and *HADHSC*, which are present in 7 overlapping pathways.

Table 3.2 Cellular and regulatory processes involving the differentially expressed hepatic genes between treatment comparisons of CS and T₃. Pathways are based on analysis with Pathway Miner as described in the text and include gene products from KEGG, BioCarta, and GenMAPP. Fold increase is based on the adjusted ratio comparison of CS versus T₃. Values highlighted in red indicate up-regulation by T₃ compared to CS, and values highlighted in yellow indicate up-regulation by CS compared to T₃.

Pathway Name	Gene Name	Fold Increase
MAPK signaling pathway		
	<i>PRKCM</i>	2.08
	<i>HSPA8</i>	2.04
	<i>IL1B</i>	1.72
	<i>CDC42</i>	1.56
	<i>ACVRIC</i>	1.52
	<i>MAPKAPK2</i>	1.25
	<i>PAK2</i>	1.21
	<i>MAPK9</i>	1.41
	<i>PRKCI</i>	1.54
Wnt signaling pathway		
	<i>FZD6</i>	2.78
	<i>PRKCM</i>	2.08
	<i>FZD1</i>	1.37
	<i>CCND1</i>	1.32
	<i>LRP5</i>	1.21
	<i>FZD2</i>	1.33
	<i>MAPK9</i>	1.42
	<i>PRKCI</i>	1.54
Ubiquitin mediated proteolysis		
	<i>FZR1</i>	3.03
	<i>CUL2</i>	1.56
Proteasome		
	<i>PSMD4</i>	2.17
	<i>PSMD2</i>	1.85
	<i>PSMD11</i>	1.39
	<i>PSMB3</i>	1.32
	<i>proteasome regulatory particle p44S10</i>	1.35
TGF-beta signaling pathway		
	<i>ACVRIC</i>	1.52
	<i>SMURF2</i>	1.24
	<i>CHRD</i>	1.32
	<i>BMP4</i>	1.50

Phosphatidylinositol signaling system	
<i>PRKCM</i>	2.08
<i>PIK4CA</i>	1.28
<i>PRKCI</i>	1.54
Gene Regulation by PPARα	
<i>EHHADH</i>	3.85
<i>ACOX1</i>	2.27
<i>CD36</i>	1.47
<i>PRKARIA</i>	1.45
Inflammatory Response Pathway	
<i>VTN</i>	3.23
<i>C3</i>	2.70
<i>COL3A1</i>	1.47
IL-10 Anti-inflammatory Signaling Pathway	
<i>IL10RA</i>	1.89
<i>HMOX1</i>	1.39
Complement Activation	
<i>C3</i>	2.70
<i>C4A</i>	2.17
<i>C8A</i>	2.13
<i>C2</i>	2.04
<i>C1S</i>	1.79
<i>MASPI</i>	1.45

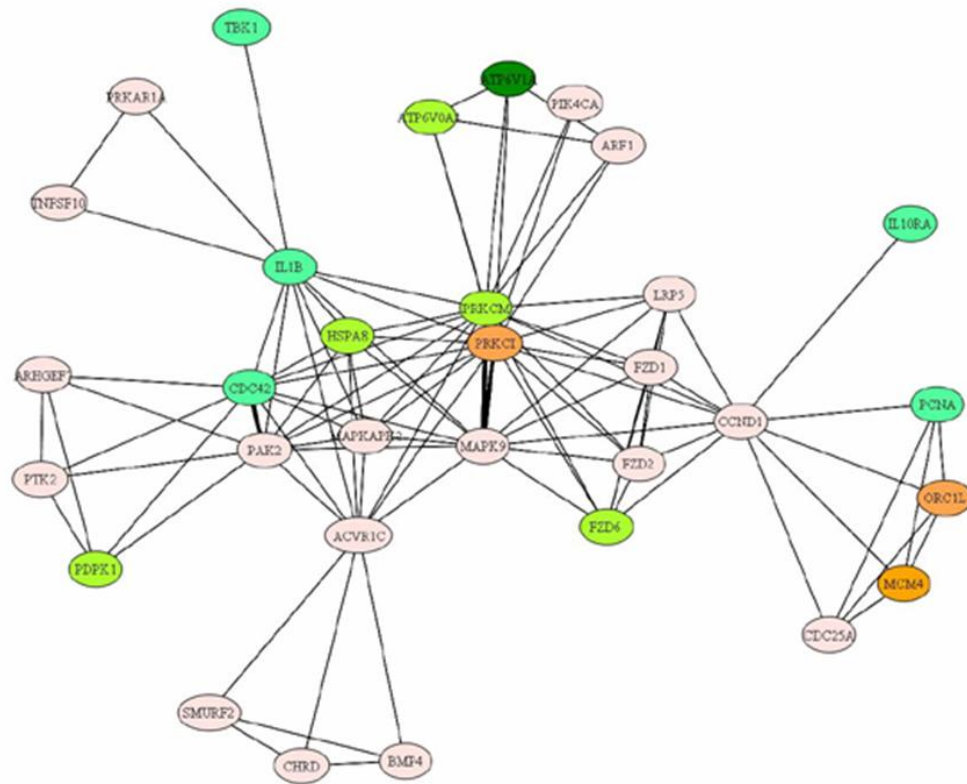


Figure 3.7 Gene association network of cellular and regulatory processes involved in the response of hepatic genes to either CS or T₃. Nodes are colored based on the expression values of genes up-regulated with T₃ (green) or genes up-regulated with CS (red). Genes that had less than 1.5 fold change in expression are represented as pink. Edge weight indicates number of co-associated pathways between genes. Nodes are labeled with gene name. Network is based on KEGG pathway resource in Pathway Miner.

Table 3.3 Metabolic processes involving the differentially expressed hepatic genes in the CS versus T₃ contrast. Pathways are based on analysis with Pathway Miner as described in the text and include gene products from KEGG. Fold increase is based on the adjusted ratio comparison of CS versus T₃. Values highlighted in red indicate up-regulation by T₃ compared to CS, and values highlighted in yellow indicate up-regulation by CS compared to T₃.

Pathway Name	Gene Name	Fold Increase
Glycolysis / Gluconeogenesis		
	<i>ALDOB</i>	3.45
	<i>ENO1</i>	3.13
	<i>PGAM1</i>	2.70
	<i>LDHB</i>	2.63
	<i>ADH1B</i>	2.33
	<i>FBP1</i>	1.75
	<i>ALDH3A1</i>	1.52
	<i>GPI</i>	1.52
	<i>PGK1</i>	1.49
	<i>PFKL</i>	1.22
	<i>DLD</i>	1.26
ATP synthesis		
	<i>ATP6V1A</i>	4.17
	<i>ATP6V0A1</i>	2.13
	<i>ATP5G1</i>	2.04
	<i>ATP5A1</i>	1.92
	<i>ATP5H</i>	1.64
Fatty acid metabolism		
	<i>EHHADH</i>	3.85
	<i>CYP4B1</i>	3.33
	<i>CYP2A6</i>	2.70
	<i>PECI</i>	2.63
	<i>ADH1B</i>	2.33
	<i>ACOX1</i>	2.27
	<i>ACSL1</i>	2.08
	<i>CYP19A1</i>	1.85
	<i>CYP2E1</i>	1.82
	<i>CYP2J2</i>	1.69
	<i>HADH2</i>	1.54
	<i>HADHSC</i>	1.45
	<i>ACAT2</i>	2.37

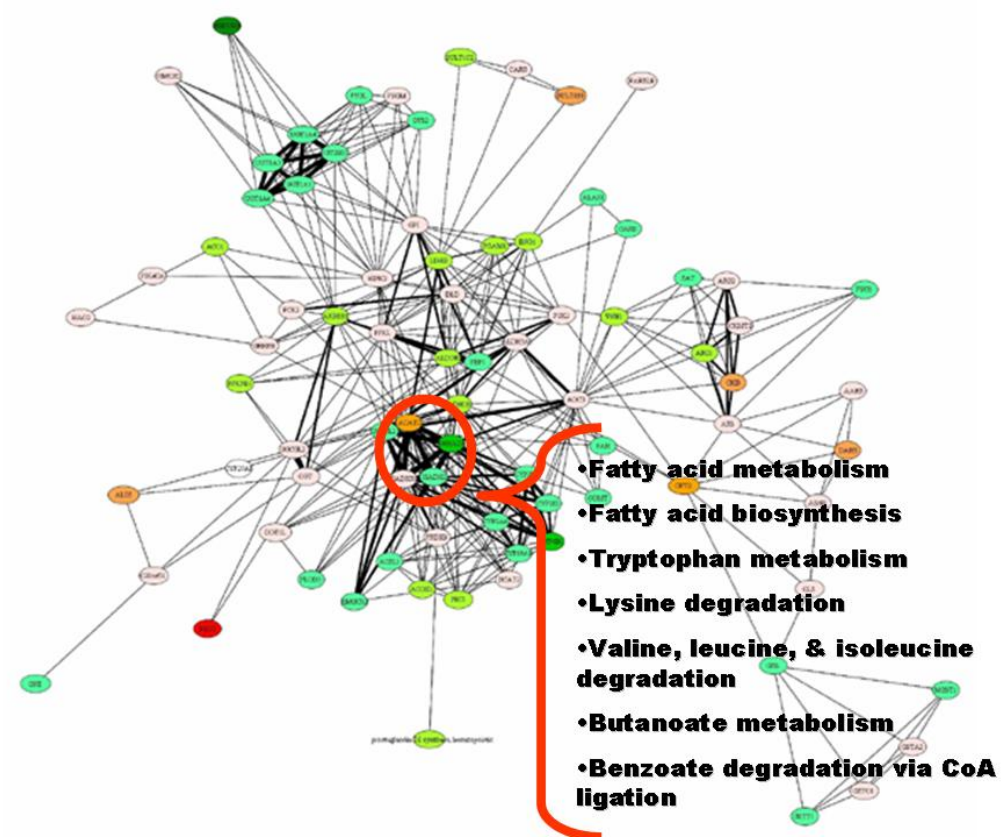


Figure 3.8 Gene association network of metabolic processes involved in the response of hepatic genes to either CS or T₃. Inset shows network association of four genes (*ACAT2*, *EHHADH*, *HADH2*, and *HADHSC*) that co-occur in 7 different KEGG pathways. Nodes are colored based on the expression values of genes up-regulated with T₃ (green) and genes up-regulated with CS (red). Genes that had less than 1.5 fold change in expression are represented as pink. Edge weight indicates number of co-associated pathways between genes. Nodes are labeled with gene name. Network is based on KEGG pathway resource in Pathway Miner.

3.4 Analysis of Expression by Real-Time Quantitative RT-PCR

In order to validate the differential gene expression revealed by the microarray data (Table 3.4), the expression of 5 genes (*APOB*, *DEFB9*, *LDHB*, *PEPCKM*, and *THRSP*) were analyzed by real-time qRT-PCR. An additional 12 genes (*ACACA*, *ADRP*, *AFABP*, *APOC3*, *FAS*, *Fath*, *LPL*, *ME1*, *PEPCKC*, *PK*, *SCD1*, and *SOD3*) were also analyzed for their expression patterns across the treatments. The expression patterns of these genes are presented in Figs. 3.9, 3.10, 3.11, 3.12, and 3.14.

CS infusion, alone or in combination with T₃, increased (P < 0.05) the expression of several genes compared with the control. These CS-responsive genes include *ADRP*, which was expressed 5.4-fold higher (P < 0.05) with CS alone and 2-fold higher with the CS+ T₃ treatment, when compared to vehicle control (Fig. 3.9A). CS and CS+ T₃ increased expression of *APOC3* which was 3- and 2-fold higher (P < 0.05), respectively, when compared to either VC or T₃ treatments (Fig. 3.9B). *PEPCKC* expression was higher (P < 0.05) under CS or CS+ T₃ treatments (Fig. 3.9C). Furthermore, all three of these genes showed no significant difference between the vehicle control and T₃ treatments. Although *AFABP* expression was greater in the CS versus VC contrast, there was no overall treatment difference (Fig. 3.9D).

Infusion of chickens with T₃ increased the expression of metabolic genes, transcription factors, and signaling and transport proteins (Fig. 3.10). The overall treatment effect on expression of *SOD3* had a significance level of P < 0.096. However, the least significant difference (LSD) contrast indicates that T₃, alone or in combination with CS, increased the expression of *SOD3* (Fig. 3.10A). *Fath* was elevated by T₃, alone, when compared to VC or CS (Fig. 3.10B). *THRSP* was elevated (P < 0.05) by all exogenous hormone treatments (Fig. 3.10C). The

combination of CS+ T₃ resulted in the highest expression of *THRSP*, which was 5.1-fold higher (P < 0.05) than the VC treatment (Fig. 3.10C). The expression of *APOB* was depressed (P < 0.05) under the CS treatment, when compared to the higher expression found with T₃, alone or in combination with CS (Fig. 3.10D).

The differential expression of four lipogenic genes was clearly demonstrated by real-time qRT-PCR analysis (Fig. 3.11). For example, *FAS* was increased 3.8-fold after 6 days of CS infusion (Fig. 3.11A). T₃, alone or in combination with CS, had no significant effect on *FAS* abundance (Fig. 3.11A). *SCD1* is another example of an important lipogenic gene, which was up-regulated by CS, alone (4.2-fold) or in combination with T₃ (3.4-fold) (Fig. 3.11B). T₃, alone, had no effect on expression of *SCD1* (Fig. 3.11B). The metabolic enzyme, *PEPCKM*, was similarly elevated by CS, alone (1.4-fold) or in combination with T₃ (1.6-fold) (Fig. 3.11C). However, microarray analysis showed that CS was down-regulated 1.4, which was the only case in which the real-time qRT-PCR data was different than the microarray data (Table 3.4). Furthermore, CS, alone or in combination with T₃, significantly increased the expression of *ACACA* 2.3-fold or 1.9-fold, respectively (Fig. 3.11D).

The differential expression of four key lipolytic genes was altered by hormonal infusion (Fig. 3.12). *PK* expression was significantly increased under T₃ treatment, whereas it was not affected by CS, alone or in combination with T₃ (Fig. 3.12A). *LDHB* expression was dramatically depressed by CS (8.6-fold) (Fig. 3.12B). The expression of *LDHB* was depressed in the CS+ T₃ treatment as compared to T₃, alone (Fig. 3.12B). CS exerted an even more dramatic depressive action on *LPL* (63-fold) (Fig. 3.12C). Similarly, CS in combination with T₃ also depressed *LPL*

expression in the liver (2.5-fold) (Fig. 3.12C). *MEI* was increased by CS, alone (2.2-fold) or in combination with T₃ (3.5-fold) (Fig. 3.12D).

Table 3.4 Select differentially expressed genes revealed by microarray analysis and verified by real-time qRT-PCR. Values indicate fold increase based on the adjusted ratio comparisons of CS versus T₃, CS versus VC, CS+T₃ versus CS, or CS+T₃ versus VC. Values highlighted in red indicate up-regulation by T₃ compared to CS, values highlighted in green indicate up-regulation by VC compared to CS or CS+T₃, values highlighted in yellow indicate up-regulation by CS compared to VC, and values highlighted in blue indicate up-regulation by CS+T₃ compared to VC or CS, respectively. Asteriks (*) indicate no significant (P < 0.05) difference between treatment contrasts.

Gene Name	CS vs. T ₃		CS vs. VC		CS+T ₃ vs. CS		CS+T ₃ vs. VC	
	Array	qRT-PCR	Array	qRT-PCR	Array	qRT-PCR	Array	qRT-PCR
<i>APOB</i>	2.1	1.8	1.8	*	*	*	*	*
<i>LDHB</i>	2.6	24.7	*	8.7	*	3.8	*	2.3
<i>PEPCKM</i>	1.5	*	1.4	1.4	2.3	*	*	1.6
<i>THRSP</i>	2.6	*	*	3.6	4.0	*	5.6	5.2

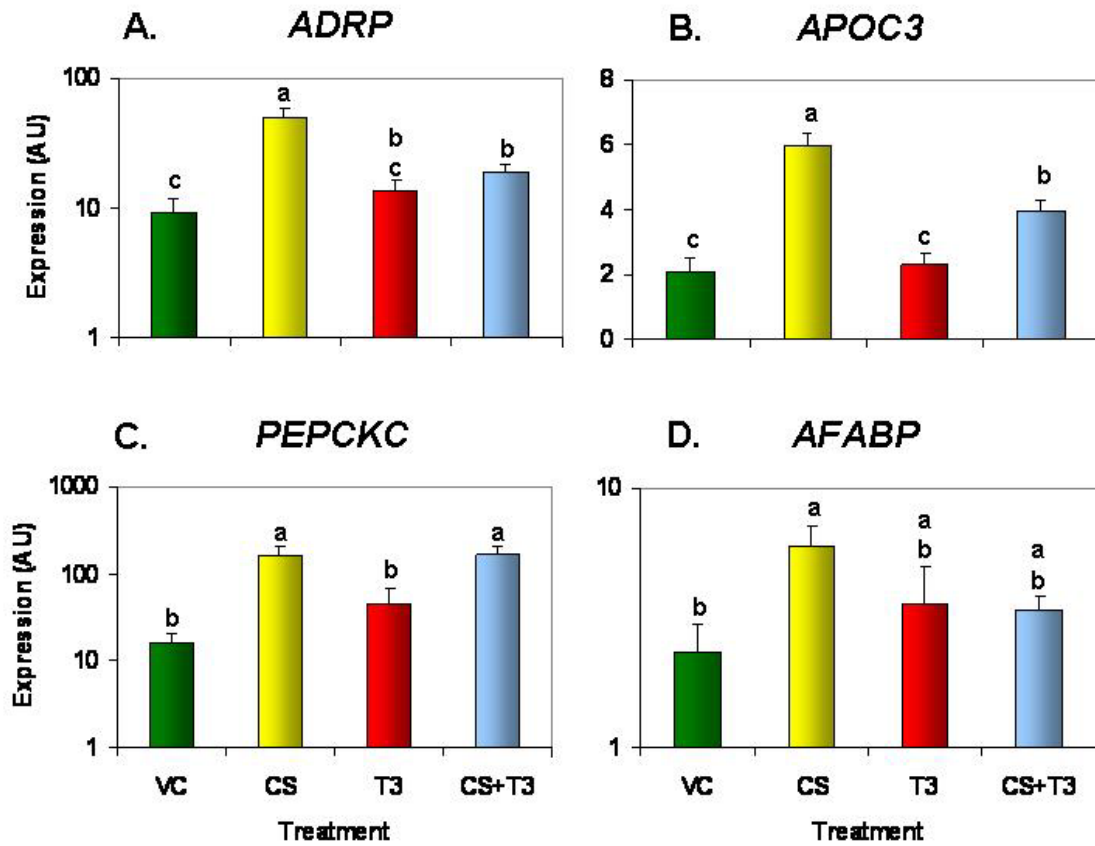


Figure 3.9 Expression of CS-responsive genes as indicated through real-time qRT-PCR. Each value [in arbitrary units (AU)] represents the mean \pm SEM of six birds per treatment (except five birds in CS+T₃). Treatments without the same superscript are significantly ($P < 0.05$) different.

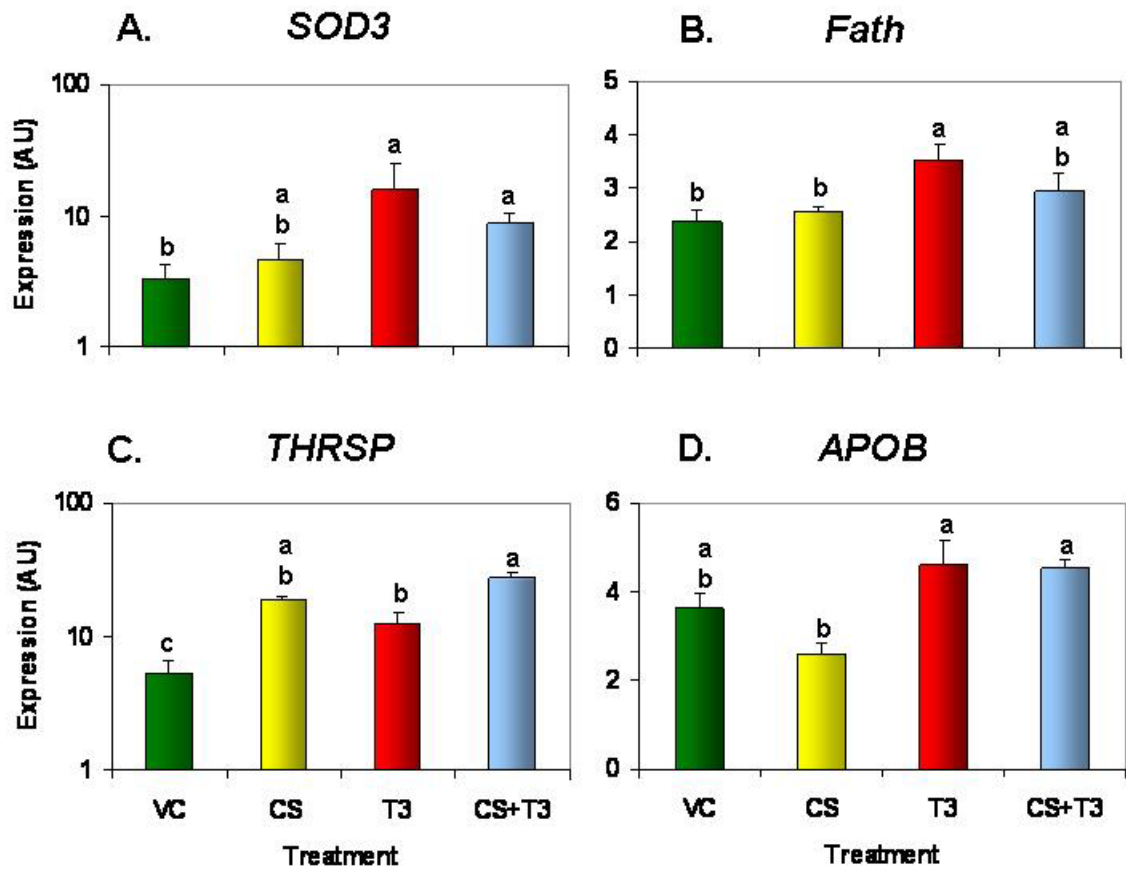


Figure 3.10 Expression of T₃-responsive genes as indicated through real-time qRT-PCR. Each value [in arbitrary units (AU)] represents the mean ± SEM of six birds per treatment (except five birds in CS+T₃). Treatments without the same superscript are significantly ($P < 0.05$) different.

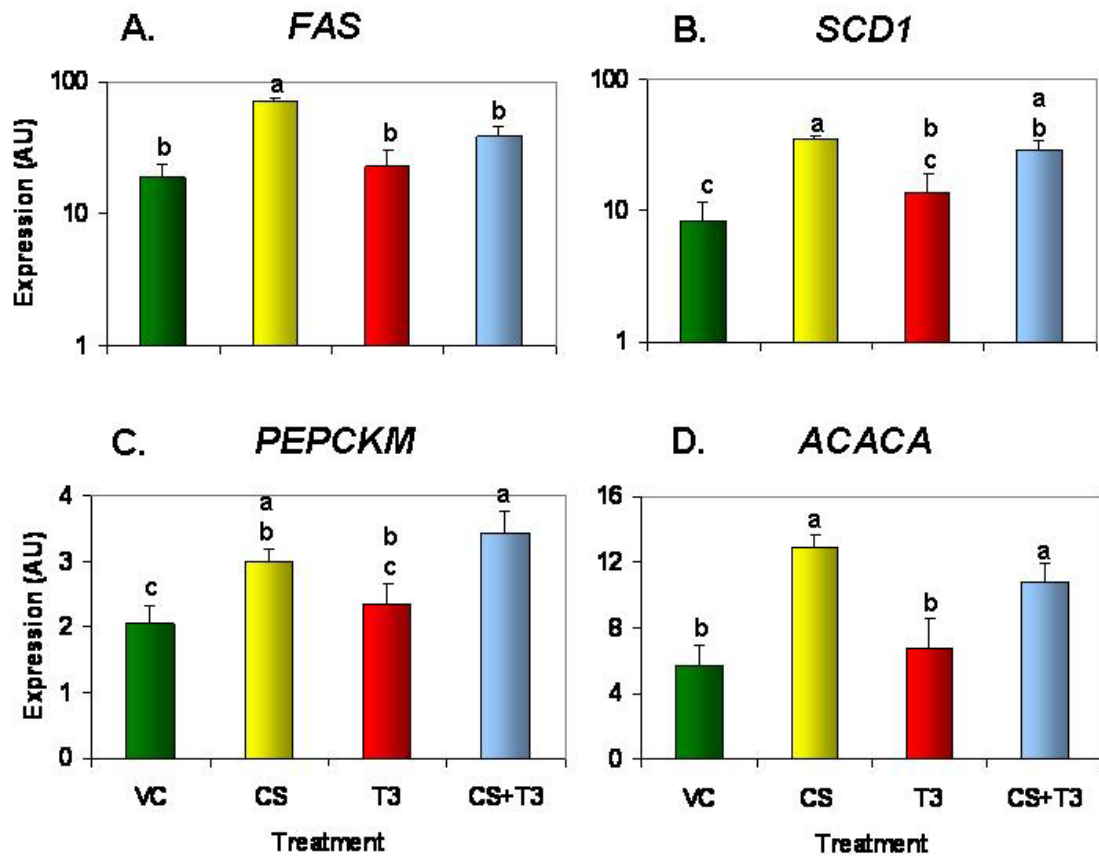


Figure 3.11 Expression of key *lipogenic* genes as indicated through real-time qRT-PCR. Each value [in arbitrary units (AU)] represents the mean \pm SEM of six birds per treatment (except five birds in CS+T₃). Treatments without the same superscript are significantly ($P < 0.05$) different.

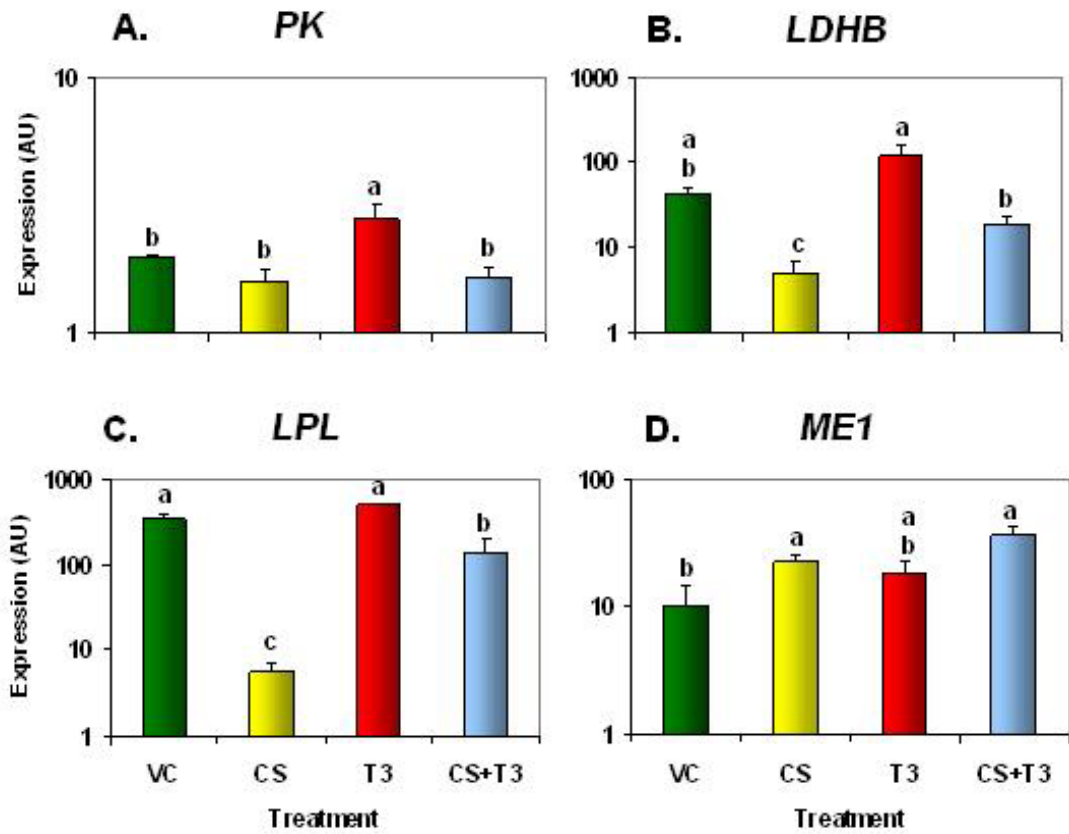


Figure 3.12 Expression of key *lipolytic* genes as indicated through real-time qRT-PCR. Each value [in arbitrary units (AU)] represents the mean \pm SEM of six birds per treatment (except five birds in CS+T₃). Treatments without the same superscript are significantly ($P < 0.05$) different.

3.5 Functional Mapping of Metabolic Pathways

The lipogenic and lipolytic differentially expressed genes (Fig. 3.11 and 3.12, respectively) were incorporated into a working pathway, which shows the effect of the exogenous hormones on glycolysis, gluconeogenesis, and glyceroneogenesis in the liver (Fig. 3.13). Exogenous CS increased the expression of three genes coding for key enzymes involved in lipid biosynthesis (*ACACA*, *FAS*, and *SCDI*). T_3 increased expression of two genes, *PK* and *LDHB*, which transcribe enzymes responsible for the generation of pyruvate from phosphoenolpyruvate (*PEP*) and lactate, respectively. This increased availability of pyruvate should drive activity of the TCA cycle and, subsequently, the generation of ATP. T_3 also increases expression of *LPL*, which is involved in the catabolic conversion of triglycerol into fatty acid. The combination of CS+ T_3 led to increased expression of two metabolic enzymes, *ME* and *PEPCKM*. Increased levels of *ME* correspond to the increased conversion of malate to pyruvate, which has a dual action in this pathway. First of all, increased activity of the TCA cycle should generate more citrate for lipid biosynthesis. Second, conversion of malate to pyruvate generates NADPH, a necessary reducing agent for the anabolic activity of *FAS* and greater fatty acid biosynthesis. Furthermore, increased expression of *PEPCKM* by CS+ T_3 leads to increased production of *PEP*, which could enhance gluconeogenesis and/or glyceroneogenesis. Increased activity of these pathways supports greater adiposity with CS, alone, and slightly less adiposity with CS+ T_3 .

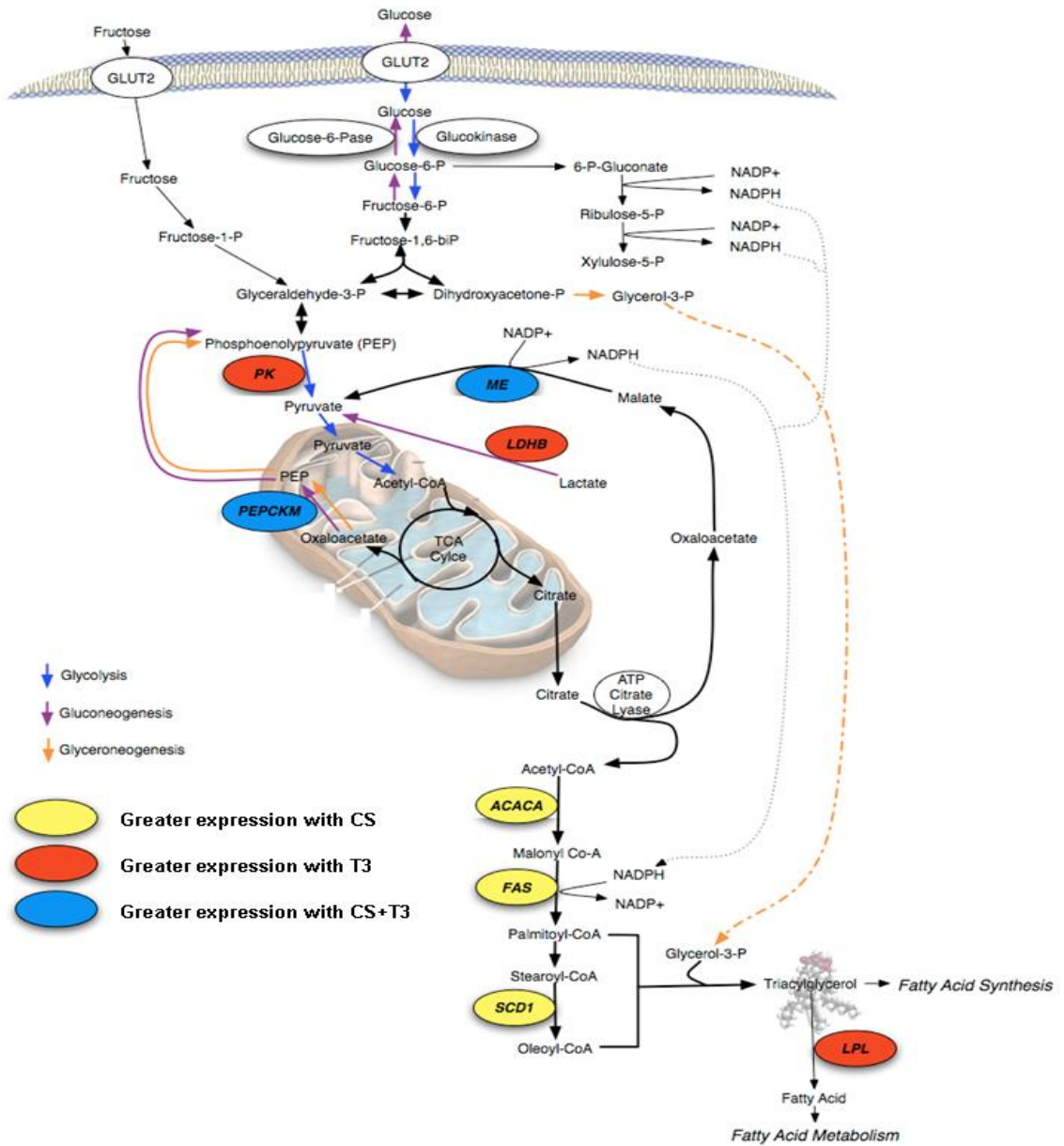


Figure 3.13 (Legend appears at top of next page.)

Figure 3.13 (*On the previous page.*) **Impact of exogenous hormones on key metabolic genes involved in metabolism and synthesis of fat.** The pathways of glycolysis (represented with blue arrows), gluconeogenesis (represented with purple arrows), and glyceroneogenesis (represented with orange arrows) function in overall lipogenesis in the chicken liver. Key genes that transcribe vital enzymes of the pathway are indicated in circles. Circles filled with yellow, red, or blue signify genes that were verified as differentially expressed through real-time qRT-PCR ($P < 0.05$) and revealed a greater expression with CS, T_3 , or CS+ T_3 , respectively. (Pathway modified from Beale et. al (39), Richards et. al (32), and Towle et al. (40).)

3.6 Identification of a Novel Obesity-Related Gene Family

Microarray analysis revealed differential expression of three members of a family of anti-microbial peptides, the β -defensins (Table 3.5). The expression of one member of this family (*DEFB9*), represented by three distinct cDNA clones, was greatly increased by exogenous CS, alone or in combination with T_3 (Table 3.5). Real-time qRT-PCR verified higher ($P < 0.05$) expression of *DEFB9* in the CS (5.8-fold) and CS+ T_3 (19.7-fold) treatments (Fig. 3.14). In contrast, two other members of this gene family (*DEFB10* and *DEFB11*) showed increased expression with T_3 , when compared to CS (Table 3.5). Thus, the β -defensins respond divergently to lipogenic (CS or CS+ T_3) and lipolytic (T_3) hormones.

Table 3.5 Differentially expressed β -defensin genes from microarray. Values indicate fold increase based on the adjusted ratio comparisons of CS versus T₃ or CS+T₃ versus T₃. Values highlighted in red indicate up-regulation by T₃ compared to CS, values highlighted in yellow indicate up-regulation by CS compared to T₃, and values highlighted in blue indicate up-regulation by CS+T₃ compared to T₃.

Gene Name	Gallinacin	Clone ID	GenBank #	CS vs. T ₃	CS+T ₃ vs. T ₃
<i>DEFB9</i>	<i>GAL6</i>	pgl1n.pk001.114	AY621324	2.72	2.38
		pgl1n.pk003.j8		3.35	2.94
		pn11s.pk002.a12		2.61	3.64
<i>DEFB10</i>	<i>GAL8</i>	pgl1n.pk015.d14	AY621312	1.60	
<i>DEFB11</i>	<i>GAL11</i>	pcolc.pk001.d9	AY621313	1.29	

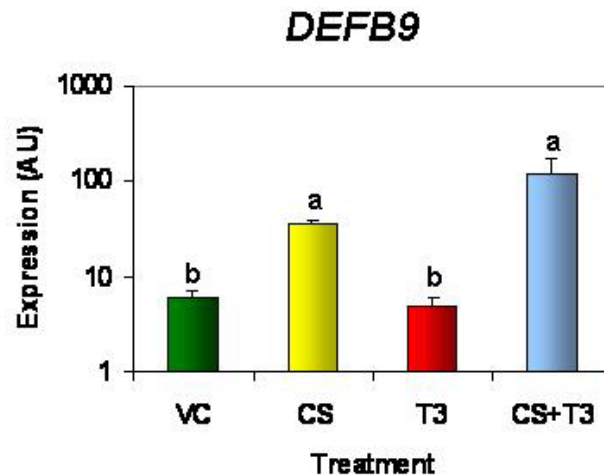


Figure 3.14 Expression of β -defensin 9 as indicated through real-time qRT-PCR. Each value [in arbitrary units (AU)] represents the mean \pm SEM of six birds per treatment (except five birds in CS+T₃). Treatments without the same superscript are significantly ($P < 0.05$) different.

Chapter 4

DISCUSSION

4.1 Phenotypic Response to Exogenous Hormones

In this study, adaptations to hormonally-induced obesity are described in liver at the molecular level. Moreover, this study shows that the expression profile related to a fat phenotype dramatically differs from that observed in lean and control groups. Due to time constraints, only the livers of Day 6 birds were used in gene expression analyses. This particular subset was chosen for further analysis, because the greatest treatment contrasts in metabolite indicators of obesity were indicated in birds after six days of treatment (Fig. 3.3). Also, this duration was half that of a previous chronic study (Fig. 1.1), thus, enabling the observance of acute regulatory genes. However, before the repercussion of these results can be fully assessed, the quality of the phenotypic changes must be addressed.

First of all, Fig. 3.1 indicates the marked increase in endogenous hormones in birds of the respective exogenous treatment group. Undoubtedly, the T_3 treatment groups, alone or in combination with CS, experienced higher levels of plasma T_3 due to hormonal infusion with subcutaneous implants of osmotic minipumps (Fig. 3.1B). Similarly, infusion with CS elevated levels of plasma CS, albeit with less obvious contrasts (Fig. 3.1A). To explain the variability in level of circulating CS from an intra-treatment perspective, a few factors must be considered. Namely, unavoidable differences in the stress incurred by the individual birds of a

treatment most likely contributed to treatment-uncharacteristic results. Although care was given to provide the same external environment and stimuli to each bird, the individual capturing and handling of each bird to obtain blood samples may have led to varied stress responses in the individual (41). Also, although one might expect to detect similar levels of corticosterone in the birds receiving either CS alone or in combination with T₃, this was not the case. However, the lower levels of CS noted in the CS+T₃ birds does not necessarily mean that the osmotic minipumps were not delivering corticosterone to these birds. In fact, the effect of T₃ treatment probably led to the decreased CS levels. Circulating corticosterone gets completely metabolized by the liver soon after its release from the adrenal glands, with a half-life of about 10-15 min in the chicken (41). The birds receiving the combined CS and T₃ treatment experienced an elevated metabolic rate due to the T₃, which, in turn, caused the circulating corticosterone (exogenous and endogenous) to be metabolized at a higher rate. This explains the lower-than-expected level of corticosterone in the double minipump birds. However, despite these lower levels, the CS+T₃ birds still had significantly higher plasma CS than those that were not receiving CS treatment. Thus, subsequent analyses can be attributable to the effects of hormonal infusion.

The plasma metabolite levels of glucose, triglycerides, and NEFA are all useful indicators of obesity. However, caution must be exercised when analyzing the results of change in glucose level to phenotypic response. The chicken is naturally hyperglycemic and has a much higher normal blood glucose concentration than mammals (42). In fact, chickens respond very poorly to large injections of insulin and are considered to be in a natural state of insulin resistance (43). With these considerations in mind, the increase in plasma glucose observed in the Day 6 CS-

treated birds is a powerful observation indicating the phenotypic pressure toward an even greater insulin-resistant state as incurred with obesity (Fig. 3.3A). Also, plasma triglyceride levels depend on the level of lipogenesis that takes place in the liver, so mild to moderate increases of plasma triglyceride levels are a good indicator of fat accretion. Furthermore, increased fat leads to increased transport of fat in the blood, which is carried out in the form of free fatty acids (NEFA). Thus, NEFA levels are effective at gauging obesity.

NEFA levels are also important in other aspects of metabolism regulation, whose dysregulation is attributed to numerous metabolic disorders. NEFA contributes to gluconeogenesis as it induces an insulin resistant state that inhibits transport of glucose and relies on the need for alternative fuel sources. This concept is slightly paradoxical in nature, because increased glucose is vital not only for the TCA cycle and production of fuel for the metabolically-active lean phenotype, but also for the increased lipogenesis causing the obese phenotype. Thus, the role of increased glucose can be shunted in either direction, toward generating obesity or toward supplying the energy needs of a higher metabolic rate. The lean phenotypic state has depleted fat stores, so they must synthesize more ATP from the TCA cycle. Although the action of lipolysis results in the direct catabolism of triglycerides into fatty acids, our “lean phenotype” induced by T_3 infusion does not cause a significant change in plasma NEFA. However, lipolysis is the inherent mode of fat reduction in the lean model, so one might expect the lean birds to have an increase in NEFA. This is not observed, because any increase in fatty acids is immediately utilized as precursors in gluconeogenesis to feed the higher metabolic rate and energy requirements.

The obese phenotype was effectively induced in CS treated birds. Results supporting this phenotypic change include the elevated feed intake without change in body weight as depicted in Fig. 3.2. Corticosterone is gluconeogenic and catabolic for muscle, which explains the maintenance of weight at control levels despite the excess feed intake. Also, this implies that the energy in excess feed was being transformed into fat. The development of an obese model is further substantiated with observations of significantly higher metabolite indicators of obesity by the CS treatment (Fig. 3.3). These results support the accepted action of pharmacological doses of glucocorticoid in increasing plasma levels of glucose and free fatty acids (44).

As far as generating a lean phenotype through exogenous T_3 treatment, the phenotypic results of the present study appear inconclusive, because of the lack of observable decrease in feed intake and body weight and/or metabolite levels (Figs. 3.2 and 3.3). However, based on the chronic study, two weeks of infusion of T_3 are effective at producing a lean phenotype, as noted in the 40% decrease in abdominal fat (Fig. 1.1). Additionally, visual inspection of the birds receiving exogenous T_3 revealed a persistent increase in respiration rate (polypnea). This was in response to the higher metabolic rate induced by T_3 , which was compensated for by increased production of CO_2 and subsequent metabolic acidosis. Furthermore, hyperthyroidism has been linked to decreased levels of plasma triglyceride due to elevated action of lipoprotein lipase in mammals (45), and a number of studies have shown a correlation between increased plasma T_3 and lower abdominal fat in chickens (46). So, although acute infusion of T_3 did not exhibit a dramatic depletion of visceral fat, as seen in the

chronic study, for all extensive purposes, the T₃ treatment group will act as the lean phenotype for contrast with the CS-induced fat phenotype.

4.2 Transcriptional Response to Exogenous Hormones

While the assumption is made that the T₃ treatment group is effectively the lean phenotype, microarray analysis and hierarchical clustering expose the inherent flaws in this assumption. Fig. 3.5 shows the clustering of microarrays by similar expression patterns. The odd clustering of slides from the T₃ treated birds reinforces the similarity of T₃ birds with the VC birds. This is further stressed in Table 3.1 and Fig. 3.4, which show that the least number of differentially expressed genes is among the T₃ versus VC contrast. On the other hand, the microarray results revealed the profound transcriptional response that CS treatment had when inducing the obese phenotype. In fact, the CS+T₃ treatment favored responses that paralleled results of treatment with CS, alone, as is indicated with the clustering relationship between CS and CS+T₃ (Fig. 3.5). However, the greatest number of differentially expressed genes belong to the CS versus T₃ contrast. Thus, although minor in phenotypic changes, the acute T₃ treatment provided a suitable opposing contrast that enabled the generation of an exhaustive list from a broader spectrum of differentially expressed genes than possible when merely comparing the fat phenotype to the non-perturbed control.

Fig. 3.5 reveals some dissimilarities among the T₃ treated birds. Of particular interest, one of the T₃ microarray slides clustered more similarly with the CS treatment group. This may in part be due to a defective or lost minipump of the respective T₃ treated bird. In fact, this bird had very low circulating plasma T₃ levels (3.26 ng/ml) as compared to the mean T₃ level experienced by birds with T₃ osmotic

minipumps (7.09 ng/ml and 6.39 ng/ml for T₃ alone and in combination with CS, respectively) (Fig. 3.1). Thus, it is necessary to question the effectiveness that the potentially inadequate T₃ treatment had on inducing the desired lean phenotype in this individual. Despite its low circulating T₃ levels, this bird was included in all subsequent analyses. Fig. 3.5 shows that among differentially expressed genes, CS down-regulated a clear majority (blue clusters). This should be kept in consideration during analysis of treatment contrasts against CS, owing differential expression to the preferential down- (blue clusters) or up-regulation (red clusters) of CS.

4.3 Clustering Differentially Expressed Genes into Functional Pathways

Microarray analysis enabled the discovery of what RNA sequences were present in the liver, which then correlated to how strongly these genes were expressed in the hepatocytes. Recognizing how genes contribute to metabolic pathways that result in phenotypic differences is an essential quest of the post-genomics era. When the expression of a particular gene changes in accordance to differing phenotypes, it can be assumed that this gene plays a particular function in regulating that phenotype, be it a causative or effective relationship. Although not all genes in a pathway can be identified through transcriptional profiles, those that are differentially expressed will enable a rough approximation of the activity of specific pathways and their regulation by transcription factors and/or enzymes.

Pathway Miner analysis allowed functional clusters of genes that responded to exogenous adrenal and/or thyroid hormone (Table 3.2). For example, the largest numbers of differentially expressed genes are assigned to six major pathways. The MAPK, WNT, TGF-beta, and phosphatidylinositol (PI3K) signaling pathways may explain the phenotypic response observed with infusion of CS or T₃.

Signaling pathways control gene activity and transcription of target genes; thus, the subsequent action of these pathways could lead to the up- or down-regulation of key genes involved in lipogenesis (CS) and increased metabolism (T_3). Pathways involved in protein turnover, such as the ubiquitin mediated proteolysis and proteasome function, include 7 differentially expressed genes. Increased protein catabolism is observed under both treatment conditions, as CS and T_3 are both gluconeogenic, although the phenotypic outcomes dramatically differ. Also, it is interesting to note that there are 11 differentially expressed genes involved in the innate immune (Complement pathway) and inflammatory response. There are members of the MAPK and TGF- β signaling that are also considered to be pro-inflammatory. This supports the idea that inflammation is an important process that leads to the development of obesity and its associated complications.

A large number of differentially expressed genes were associated with three major metabolic processes (glycolysis/gluconeogenesis, ATP synthesis, and fatty acid metabolism) identified through Pathway Miner analysis (Table 3.3). The importance of glycolysis and gluconeogenesis in sustaining the phenotypic responses is illustrated by the presence of a large number of metabolic enzymes, and the significance of these pathways on lipogenesis and lipolysis are discussed below. T_3 infusion caused the up-regulation of 5 genes involved in ATP synthesis, which is necessary for maintaining the high metabolic rate of birds receiving exogenous T_3 . Fatty acid metabolism has a seemingly obvious role in generating the obese or lean phenotype. For instance, the only CS up-regulated gene included in this category is acetyl-Coenzyme A acetyltransferase 2 (*ACAT2*), which is involved in cholesterol transport and is also present in human liver and implicated in atherosclerosis (47).

The large number of T₃-induced genes in this category suggests the high rate of fat breakdown in the lean phenotype. The cluster identified in the network of metabolic processes (Fig. 3.8) contains four genes that are involved in 7 co-associated pathways, which include fat and amino acid metabolism. Three genes in this cluster (*EHHADH*, *HADH2*, and *HADHSC*) are involved in beta-oxidation of fatty acids, which is elevated by exogenous T₃. The only CS up-regulated gene was *ACAT2*, which is a key factor in cholesterol transport and lipoprotein metabolism in humans (47).

Finally, it should be noted as a caveat that although the results indicate that most of the differentially expressed genes are involved in metabolism (Fig. 3.6B), this may, in fact, be misleading. One must take into account the nature of probes spotted on the microarray, which are predominantly genes derived from metabolic and somatic tissues (10). Thus, it is no wonder that corresponding analysis favored metabolically-relevant genes. To avoid this bias, future studies would benefit from a more global gene analysis with genome-wide arrays that include genes spanning a larger number of molecular functions and biological processes (48). One such commercially available array is the GeneChip® Chicken Genome Array (Affymetrix).

4.4 Real-Time qRT-PCR Verification of Obesity-Related Genes

4.4.1 Transport Proteins

Glucocorticoids have been reported to affect the expression of genes coding for a number of apolipoproteins (44). Apolipoproteins play a role in transporting lipids in plasma from the liver to target tissues. Apolipoprotein CIII (*APOC3*) is a potent inhibitor of lipoprotein lipase, delaying catabolism of

triglycerides, and promoting hypertriglyceridemia (49). This inverse relationship between *APOC3* expression and lipoprotein lipase (*LPL*) expression was observed in the CS and CS+T₃ treated birds (Figs. 3.9B and 3.12C, respectively), which helps explain the greater adiposity in these birds. The expression of *APOB* is decreased by treatment with CS, alone, in contrast with T₃, alone or in combination with CS, and there is no significant difference between *APOB* expression in the CS versus VC contrast (Fig. 3.10D). These observations seem to contradict the purported relationship between high *APOB* levels and obesity (50). However, Smith et al. comment that the overall understanding of *APOB* and its relationship with obesity and type 2 diabetes remains far from complete (50). As a point of contention, the Pima Indians in Arizona, a population rampant with obesity and type 2 diabetes, actually have quite normal levels of plasma apoB (50). Clearly, the role of *APOB* in development of obesity requires further study.

Adipocyte fatty acid binding protein (*AFABP*) and adipose differentiation-related protein (*ADRP*) underwent similar expression level changes in presence of CS treatment (Figs. 3.9A and 3.9D). Both proteins encoded by these genes are involved in lipid metabolism, so their increased expression would be expected in the obesity-induced phenotype. Hepatic expression of FABP has been shown to increase in birds fed ad libitum compared to feed restricted birds during peak egg production (32). Chang et al. look at the importance of *ADRP* in triglyceride accumulation and show the reduction of plasma triglyceride in mice with inactivated *ADRP* (51). Also, the results of the present study agree with the recent report of Wang et al., where hepatic *ADRP* expression is elevated in chickens with increased fat deposition due to PTU-induced hypothyroidism (30).

4.4.2 Transcription Factors

Transcription factors represent a very interesting functional gene group, because many are activated by ligand-activated nuclear receptors, which upon activation bind to complexes in their promoter regions. The transcription activating ligands include metabolites, glucose, carbohydrates, sterols, retinols, and lipid soluble hormones (i.e., CS and T₃). Thyroid hormone responsive Spot 14 (*THRSP*) was revealed to be differentially expressed through microarray analysis and then verified through real-time qRT-PCR analysis, where all hormonal treatments caused elevation of expression of *THRSP* compared to vehicle control (Fig. 3.10C). *THRSP* transcribes a hepatic nuclear protein that increases in presence of T₃, glucose, and insulin (52) and is suspected to regulate the expression of a number of lipogenic genes (21). Implications for its role in lipid biosynthesis stem from observations that the expression profile of *THRSP* is similar to that of genes involved in fat deposition (21). Fig. 3.10C shows that expression of *THRSP* increases in response to T₃, alone or in combination with CS. These findings are similar to a study by Wang et. al (19), where T₃ treatment increased expression of hepatic *THRSP*. In fact, the promoter region of *THRSP* contains three thyroid response elements (TREs) which act to enhance expression of *THRSP* in response to higher T₃ (53). The present study would suggest that there is also a glucocorticoid response element, since the transcription of *THRSP* is elevated by exogenous CS, alone or in combination with T₃. The greater expression of *THRSP*, which is implicated in lipogenesis, helps contribute to higher visceral fat in the obese CS and CS+T₃ birds. Although it may seem odd that the lean phenotype birds (T₃, alone) have an increased expression of this fat-inducing transcription factor, a plausible explanation relates the gluconeogenic activity of T₃ and the need for alternative forms of energy to sustain a higher metabolic rate. Thus, the lean birds

could be utilizing the lipogenic ability of increased *THRSP* to provide fatty acid substrates necessary for gluconeogenesis. Regardless of the opposite phenotypic outcomes, this study provides additional support for the role of *THRSP* as a candidate gene in obesity. An mRNA differentially expressed in liver of genetically lean or fat line of chickens was identified as a chicken homolog of rat Spot 14 (54).

4.4.3 Metabolic Enzymes

Superoxide dismutase 3 (*SOD3*) and fat 1 cadherin (*Fath*) are excellent candidates for T₃-responsive genes involved in fat depletion. The expressions of these genes were elevated by treatment with T₃ (Figs. 3.10A and 3.10B). An increase in expression of *SOD* has also been observed in T₃ treated rats (55). This gene encodes an enzyme that responds to oxidative stress, so it is tempting to speculate its involvement in reducing the superoxide radicals produced by the T₃-induced increase in metabolic rate. In fact, a positive correlation has been shown between superoxide dismutase activity and metabolic rate in rodents and primates (56). *Fath* (or *FATI*) was first identified in *Drosophila melanogaster*, where it suppresses fat tumor formation (57). It is also known for its role in cell communication. Recently, *Fath* was identified as a differentially expressed gene in liver of fast-growing chickens, which have a higher body fat content and it is located in the QTL for fatness on GGA4 in the fast-growing and slow-growing F₂ resource population (58).

The differential expression of PEPCKC in the liver samples of these hormonally treated birds signifies its importance in fat accretion. This is because under normal conditions the avian liver predominantly contains the PEPCKM isoform of this gene variant, with little to no expression of PEPCKC. The undetectable levels of hepatic PEPCKC under normal conditions are a result of the preferential mode of

gluconeogenesis through oxidation of lactate in the chicken. However, under hormonal perturbation, the otherwise negligible PEPCKC can become activated or suppressed. A number of transcriptional response elements have been noted in the promoter region of avian PEPCKC, including an insulin response element that inhibits expression of the gene. Interestingly, avian PEPCKC is not known to have response elements sensitive to thyroid hormone or glucocorticoid, as are seen in the rat form of PEPCKC (59). However, the marked increase in expression of PEPCKC by CS, alone or in combination with T_3 (Fig. 3.9C), would suggest that response elements for these hormones might also be present in the avian homologue. In fact, Savon et al. alludes to a putative glucocorticoid regulatory element in the promoter of avian PEPCKC that may aid in the induction of its transcription (59). The gluconeogenic effect of PEPCKC would help explain the increased blood glucose levels observed in the CS treated birds. Regardless, the elevated expression of both PEPCKC and PEPCKM by exogenous corticosterone signifies the importance of this enzyme in lipogenesis. Furthermore, the discovery of SNPs in the promoter region of PEPCKC in humans has led to its implication as a candidate gene in type 2 diabetes, a resulting complication of the metabolic syndrome (60). All together, the present findings help support the role of *PEPCK* in these metabolic disorders.

In addition, Beale et al. call attention to the glyceroneogenic action of PEPCKC in the liver (39). Glyceroneogenesis is the pathway by which triglyceride is formed from gluconeogenic precursors through the intermediate synthesis of G3P (see Fig. 7). It is the increased and decreased expression of PEPCKC on glyceroneogenesis that may lead to its role in obesity and type 2 diabetes, respectively

(39). Also, Beale et al. suggest that *PEPCKM* may work through similar mechanisms and its contribution to obesity should not be overlooked.

Four lipogenic (Fig. 3.11) and four lipolytic (Fig. 3.12) genes, verified through real-time qRT-PCR, were depicted for their interactions and role in fat biosynthesis and/or metabolism in Fig. 3.13. The fat phenotypic response was partly influenced by increased expression of acetyl-coenzyme A (*ACACA*), fatty acid synthase (*FAS*), and delta-9-desaturase (*SCD1*). Richards and colleagues have implicated the importance of these genes in lipogenesis and found a high correlation (about 80-90%) between the hepatic expression levels of these genes in broiler chickens (32). They also found the expression of *LPL* to be similar to the expression of lipogenic genes. However, the present study found expression of *LPL* to be highly depressed by CS treatment, alone or in combination with T_3 (Fig 3.12C). The expression of lactate dehydrogenase B (*LDHB*) showed a similar dramatic decrease by CS (Fig. 3.12B). *LDHB* is thought of as a thyroid hormone responsive gene and has been shown to increase in hyperthyroidism (30). Both *PEPCKM* and malic enzyme 1 (*ME1*) showed the greatest expression under CS+ T_3 treatment (Figs. 3.11C and 3.12D), indicating the lipogenic properties of these genes. *ME* generates the reducing agent, NADPH, which favors the reductive anabolic pathways of fatty acid synthesis and has heretofore been shown to increase expression under an obese phenotype (32). The expression of pyruvate kinase (*PK*) was elevated by T_3 infusion, suggesting its importance in sustaining the lean phenotype by catalyzing the TCA cycle and production of ATP. The roles of these lipogenic and lipolytic genes in the pathway outlined in Fig. 3.13 provide a better understanding of the mechanisms guiding fat accumulation and metabolism.

The microarray and RT-PCR data are consistent with differential expression of several CS and T₃ responsive genes. *FAS* contains glucocorticoid regions that stimulate expression of *FAS* in presence of dexamethasone, but are antagonized by T₃ (61). Polyunsaturated fatty acids, which induce fatty acid oxidation, have been reported to decrease expression of *FAS* and *THRSP* (62). T₃ treated cells of a rat pituitary cell line showed differential expression of several genes that suggested silencing of the WNT signaling pathway (55). The same study showed increased expression of *SCD1*, *FAS*, *SOD*, *LDH*, *PEPCK*, and *PK*. Analysis of rat liver expression patterns revealed that T₃ treated rats had increased expression of *ADRP*, *FAS*, *LPL* and *THRSP* (63). Treatment with methylprednisolone, a glucocorticoid, caused differential gene expression in rat liver, including up-regulation of *LPL*, genes involved in MAPK signaling, protein kinase, and proteasome activity, and down-regulation of *ADRP*, *APOB*, *APOC3*, *FAS*, and *SCD1* (64). Oddly, these results are the opposite of the findings presented for chickens in the present study. Additional studies by Yen et al. also identified a number of thyroid hormone responsive genes that were involved in gluconeogenesis, lipogenesis, insulin signaling, and cellular immunity (65).

4.5 Avian β -Defensin: Its Evolutionary Role and Implication in Obesity

The significant up-regulation of β -defensin 9 (*DEFB9*) noted in the treatment contrast of CS, alone or in combination with T₃, versus T₃, alone, and the peculiar contrasting down-regulation observed in *DEFB10* and *DEFB11* (Table 3.5 and Fig. 3.14) encourages further review of the importance of β -defensins in the phenotypic response. Recent studies by Carre et al. (54;66) and Wang et al. (30) have brought attention to avian β -defensin 9 and its regulation of adiposity. Although its

specific role in obesity is still under question, an intense investigation of the molecular evolution and biological role of the β -defensin family is necessary. This will hopefully lead to further insight into the importance of avian β -defensin as it relates to the global epidemic of human obesity.

Carre et al. (54) made an important discovery of a polymorphism between lean and fat chickens on a heretofore “unknown” gene, whose function in obesity was merely speculative. Upon analysis of hepatic RNA from chickens divergently selected for leanness and fatness, a gene expressed solely in the liver was identified by differential display analysis to have two single nucleotide polymorphisms (SNP) in its purported coding region. Further examination indicated that these palindrome polymorphisms occurred at position 263 and 299 of EST’s GAR120-C6-2C and GAR33-G5-5B, with a fat-specific mRNA (C₂₆₃ and T₂₉₉) and a lean-specific mRNA (T₂₆₃ and C₂₉₉), respectively. The EST encoding this unknown gene was analyzed for its expression in cultured hepatocytes and Leghorn male hepatoma cells in the presence of thyroid hormone (T₃) or a synthetic glucocorticoid (dexamethasone). Northern blot analysis revealed that T₃ decreased expression of the gene, whereas dexamethasone caused a strong increase in expression (66). These findings, in combination with results from a hyperthyroid/hypothyroid study in chickens, whereby hyperthyroid (T₃-fed) chickens expressed higher levels of the unknown EST, led to the premature naming of the gene as thyroid hormone-repressible gene (*THRG*) (29;30). Cogburn et al. (29) called attention to the importance of this gene as a candidate in obesity and necessitated its further classification.

Carre et al. (66) attempted to analyze the sequence information of this unknown EST, but failed to find a match with known gene or protein sequences in

public databases. However, upon analysis of the open reading frames (ORF) in the sequence, they noted the presence of a β -defensin motif. But without support from sequence analysis, they were unable to confidently characterize the gene as a member of the β -defensin family. Only with recent identification of avian β -defensin gene sequences to EST and genomic sequence databases has the true identity of this EST been identified as Gallinacin 6, having sequence homology to human β -defensin 9 (67;68).

Defensins belong to a family of antimicrobial peptides that are part of the innate immune response to a broad spectrum of host-invasive prokaryotic and eukaryotic organisms, which include Gram positive and negative bacteria, fungi, and enveloped viruses (69). They were first identified nearly forty years ago, when “lysosomal cationic proteins” in rabbit and guinea pig polymorphonucleated neutrophils were reported as providing defense against microbes (70). The first β -defensin to be characterized was of bovine tracheal epithelial origin (71), and in 1998, hBD-2 was discovered as the first human β -defensin transcriptionally-regulated in response to microbial attack (72). Other classes of antimicrobial peptides have been identified in insects and amphibians. Cecropins, although originally identified in insects as potent antibacterial peptides, have also been found in porcine intestine, implying their evolutionary conservation across a wide range of species. Also, magainins are antimicrobial peptides that were first discovered in the skin of *Xenopus*. Additional peptides have been found in other insects, barley, and horseshoe crabs (73). The earliest discovery of transcriptionally-controlled antimicrobial peptides was thionins in plants (74).

Martin et al. (75) hypothesized that the peptide's mode of antibacterial defense relies on its affinity for the anionic character of its target, such as teichoic acid and phospholipids, and that it destroyed its host by insertion into the cell membrane through specific interactions with its amphiphilic β -sheet. They proposed that β -defensins attacked in a manner similar to the mode of action of classical defensins. The cationic character of the peptide's arginine residues form electrostatic interactions with the anionic head groups of the bacterial invader and facilitate initial contact (70). Next, an electromotive force on the microbial membrane pulls the hydrophobic face of the defensin dimer into the cell (75). The final destruction of the invader is enacted through the aid of several defensin dimers that form a voltage-gated channel in the target's membrane, resulting in increased permeability of the membrane and death of the cell (75;76). An increase in positive charge of the peptide is found to increase its ability to defend the host against microbial pathogens (74).

Avian β -defensins share similar features with human and bovine β -defensins, such as homologous pairing between the six cysteine residues to form specific disulfide bonds and the presence of a conserved glycine residue (76;77). As compared to mammalian defensins, avian defensins maintain cationic character through incorporation of numerous arginine, lysine, and cysteine residues (76). Avian antimicrobial peptides have been identified from two sources, namely heterophil and non-heterophil (77). The avian heterophil β -defensins consist of 39 amino acid residues and their importance in the innate immune response has received considerable discussion (76;77). Avian heterophils lack commonly employed oxidative mechanisms as antimicrobial activity, so they must rely heavily on non-

oxidative mechanisms to destroy bacteria, such as lysozymes, cationic proteins, and peptides (76).

Human chromosome 8p22-23 is the main β -defensin locus, which, under the pressures of positive selection, has undergone duplication and divergence to yield 5 paralogous genes (78). Xiao et al. (67) reported the identification of 13 avian β -defensin genes forming a single cluster located on GGA3 (q3.5-q3.7). Upon extensive database searches of GenBank, they discovered these 13 genes, known as *Gallinacin* 1-13. Through comparative phylogenetic analysis, they suggested that chicken β -defensins and mammalian β -defensin homologues have evolved from a common β -defensin ancestor, but due to clustering of some chicken defensins with mammalian defensins, they hypothesize that the duplication of β -defensin genes probably occurred before the split between birds and mammals. The phylogenetic relationships between β -defensins of different vertebrates are depicted in Fig. 4.1.

Independently, Lynn et al. (68) discovered 7 novel avian antimicrobial peptides through homology searches of chicken EST databases and genomic sequences. Interestingly, they report the finding of Gal-10 to have a synonymous nucleotide change from C to T at position 159. If this synonymous change has a functionally relevant impact on the protein encoded by the gene, then it is possible to speculate that this SNP could have drastic changes on phenotype, such as that discovered with the lean and fat divergently selected lines of chickens as analyzed by Carre et al. (54). Could an entire family of β -defensin genes be implicated in polymorphic changes leading to obesity? Also, Lynn et al. (68) report positive selection at several amino acid sites of the mature domain and suggest that this

adaptive evolution was in response to facing new ecological niches with different microbial flora.

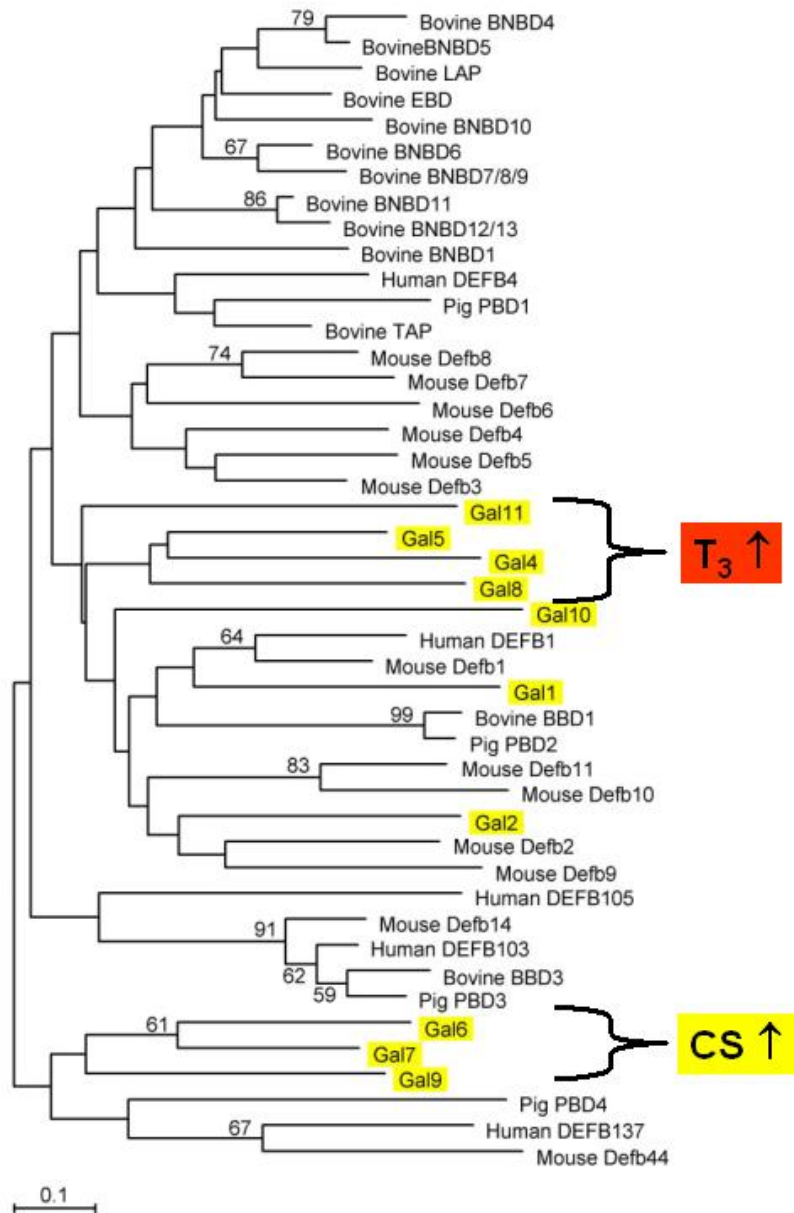


Figure 4.1 Phylogenetic relationship of vertebrate β -defensins, with chicken β -defensins on GGA3 highlighted in yellow. Gallinacin 11 (*Gal11*) and Gallinacin 8 (*Gal8*) were revealed to be up-regulated by acute infusion with T_3 , so are indicated by the T_3 cluster. Gallinacin 6 (*Gal6*) was revealed to be up-regulated by acute infusion of CS and CS+ T_3 , so is indicated by the CS cluster. [Adapted from Xiao et al. (67)].

In addition to the exhaustive role that cationic antimicrobial peptides play in the destruction of microorganisms, their importance in other innate immune response has also been elaborated on by Sugiarto and Yu (77). These additional duties include reduction of inflammation, chemotactic recruitment of other leukocytes, and wound healing. Microorganisms induce a host inflammatory response upon contact with lipopolysaccharides from Gram-negative bacteria or lipoteichoic acid from Gram-positive bacteria, which cause the release of pro-inflammatory cytokines, such as TNF- α , IL-1 β , and IL-6. Defensins inhibit this response through electrostatically interfering with the responsible bacterial factors (lipopolysaccharides and/or lipoteichoic acid). Anti-inflammatory response can be further mediated through recruitment of leukocytes (neutrophils, macrophages, T-cells, etc.), which also aid in the host initiative to destroy the pathogens. In addition, the role of antimicrobial peptides in healing damaged tissue through recruitment of fibroblasts has been proposed (77). Thus, defensins can aid in immune defense through direct interaction with the invading microorganism or through a secondary innate cellular-adaptive response (71).

Since β -defensins have been implicated in the anti-inflammatory response, it is tempting to speculate the involvement of β -defensin in obesity. Not only do they serve as stores for triglycerides, but adipocytes also play a dynamic role in the secretion of proteins involved in number of functions, including inflammation (79). The overproduction of cytokines (TNF- α , IL-6, IL-1, etc.) and adipokines (leptin, adiponectin, etc.) have been shown to aggravate symptoms of obesity (80). Tumor necrosis factor- α (TNF- α), a cytokine involved in the pro-inflammatory response, has been implicated in insulin resistance, which is strongly associated with obesity, and, in

fact, the level of TNF- α has been shown to increase in patients with obesity and/or type 2 diabetes (79). TNF- α may lead to insulin resistance through stimulation of adipocyte apoptosis and, hence, causing raised fatty acid levels. Adiponectin, another adipokine, is purported to have anti-inflammatory properties (79). Also, Bastard et al. (81) support findings that suggest a relationship between obesity and sub-clinical inflammation of adipose tissue. In fact, they also note the effect of decreased weight with reduction in inflammatory factors associated with adipose tissue. In an additional study by Lee et al. (82), they found that the most differentially expressed genes of abdominal fat tissue between obese and non-obese Pima Indians belonged to the inflammation/immune response, including genes encoding chemotactic factors for recruitment of monocytes/macrophages, members of the complement system, and C1q and tumor necrosis factor related protein 5 (*CIQTNF5*). The present study indicated with microarray analysis the increased expression (4.4-fold) of C1q and tumor necrosis factor related protein 7 (*CIQTNF7*) by CS+T₃ in contrast with VC. Furthermore, a large number of complement factors were up-regulated by T₃ in the present study (Table 3.2). Due to poorly understood mechanisms, Lee et al. (82) called for the need to further investigate the role of inflammation in adipose tissue and obesity. Evans and colleagues further describe the importance of targeting chronic inflammation in the battle against obesity and insulin resistance (4).

Through looking at our evolutionary history with other species, we can better understand ourselves, which has major implications for the treatment and diagnosis of disease. By recognizing the importance of β -defensin as an ancient, conserved response of the innate immune system, recent findings of its induced expression in obese avian models are approached in a comparative light. The initial

finding of differential expression of a gene coding for an antimicrobial peptide between lean and fat populations was viewed with much skepticism. However, its additional function in the anti-inflammatory response may allude to its relationship with obesity. Through down-regulation of cytokines, β -defensins may act to counter the effects of an inflammatory-like state of obesity. However, it is not known if increased levels of β -defensin is the result of the pathology, or if its increased expression causes the subsequent phenotypic effect. Regardless of its mode of action, this provides a new model for β -defensin's role in obesity and necessitates further studies to elucidate its relationship to fat accumulation. Additionally, the importance of β -defensin as an evolutionary conserved gene, if indeed proven to play a part in obesity, could facilitate biomedical approaches for handling the global epidemic of obesity.

This study has revealed three unique β -defensins, which show differential expression to response to exogenous adrenal or thyroid hormones. For example, *DEFB9* expression is up-regulated *in vivo* by CS (Table 3.5 and Fig. 3.14), or *in vitro* by dexamethasone, or fatty acid analogue (54;66). In contrast, the expression of *DEFB10* and *DEFB11* are depressed by CS, or elevated by T_3 . Interestingly, they belong in two distinct phylogenetic clusters (Fig. 4.1). This suggests that evolutionary divergence could account for their divergent response to either adrenal or thyroid hormone. Moreover, the discovery of the differential expression of this gene family opens a wide set of opportunities to investigate putative new gene targets to prevent or correct obesity and its associated complications.

Chapter 5

CONCLUSIONS

This study demonstrates the power of combining hormonal manipulation and microarray analysis to unravel genetic circuits that control energy metabolism and fat deposition. Perturbation of metabolism with infusion of corticosterone (CS) and/or metabolically active thyroid hormone (T_3) had a profound effect on the expression of key regulatory and metabolic genes in the liver of the chicken. A large number of CS-responsive and T_3 -responsive genes were identified through transcriptional analysis of liver samples. As expected, exogenous CS led to an obese phenotype, as indicated by elevated plasma metabolites, and increased expression levels of several transport proteins, transcription factors, and metabolic enzymes, which support lipid biosynthesis and excessive fat accretion. On the other hand, acute infusion with T_3 increased metabolic rate, lipolysis, and protein turnover. The T_3 -mediated metabolic responses were supported by altered expression of key genes in several pathways (glycolysis/gluconeogenesis, ATP synthesis, fat metabolism, etc.). The combination of exogenous CS and T_3 also revealed differential gene expression, either an additive or a dampened response when compared to either hormone alone. Moreover, the discovery of differential expression of three members of the β -defensin family in response to a lipogenic (CS) or lipolytic (T_3) hormone expands the functional role of these anti-microbial peptides. The importance of inflammation and the innate immune response in development of visceral obesity is demonstrated by identification of several genes involved in these responses. This functional genomics study promotes the chicken as a model for the study of obesity and type 2 diabetes in humans.

REFERENCE LIST

1. **Unger RH** 2003 Lipid overload and overflow: metabolic trauma and the metabolic syndrome. *Trends Endocrinol Metab* 14:398-403
2. **Moller DE, Kaufman KD** 2005 Metabolic syndrome: A clinical and molecular perspective. *Ann Rev Med* 56:45-62
3. **Beaven SW, Tontonoz P** 2006 Nuclear receptors in lipid metabolism: targeting the heart of dyslipidemia. *Annu Rev Med* 57:313-329
4. **Evans JL, Youngren JF, Goldfine ID** 2004 Effective treatments for insulin resistance: trim the fat and douse the fire. *Trends Endocrinol Metab* 15:425-431
5. **Perusse L, Rankinen T, Zuberi A, Chagnon YC, Weisnagel SJ, Argyropoulos G, Walts B, Snyder EE, Bouchard C** 2005 The human obesity gene map: the 2004 update. *Obesity Research* 13:381-490
6. **Sharma AM, Chetty VT** 2005 Obesity, hypertension and insulin resistance. *Acta Diabetol* 42:S3-S8
7. **Eckel RH, Grundy SM, Zimmet PZ** 2005 The metabolic syndrome. *Lancet* 365:1415-1428
8. **Stern CD** 2005 The chick: A great model system becomes even greater. *Devel Cell* 8:9-17
9. **Stern CD** 2004 The chick embryo - past, present and future as a model system in developmental biology. *Mech Dev* 121:1011-1013
10. **Cogburn LA, Wang X, Carre W, Rejto L, Aggrey SE, Duclos MJ, Simon J, Porter TE** 2004 Functional genomics in chickens: development of integrated-systems microarrays for transcriptional profiling and discovery of regulatory pathways. *Comp Funct Genom* 5:253-261

11. **International Chicken Genome Sequencing Consortium** 2004 Sequence and comparative analysis of the chicken genome provide unique perspectives on vertebrate evolution. *Nature* 432:695-716
12. **Schmutz J, Grimwood J** 2004 Genomes: Fowl sequence. *Nature* 432:679-680
13. **Dodgson JB** 2003 Chicken genome sequence: a centennial gift to poultry genetics. *Cytogenet Genom Res* 102:291-296
14. **Carre W, Wang X, Porter TE, Nys Y, Tang J-S, Bernberg E, Morgan R, Burnside J, Aggrey SE, Simon J, Cogburn LA** 2006 Chicken genomics resource: sequencing and annotation of 35,407 chicken ESTs from single and multiple tissue cDNA libraries and CAP3 assembly of a chicken gene index. *Physiol Genomics* (in press):
15. **Huang X, Madan A** 1999 CAP3: a DNA sequence assembly program. *Genome Res* 9:868-877
16. **Carre W, Niu Y, Gao GR, Cogburn LA** 2003 The chicken gene index: CAP3 sequence assembly and applications for functional genomics. *Proceedings Plant and Animal Genome XI Conference, San Diego, CA*
http://www.intl-pag.org/11/abstracts/P01_P61_XI.html:
17. **Cogburn LA, Wang X, Carre W, Rejto L, Porter TE, Aggrey SE, Simon J** 2003 Systems-wide chicken DNA microarrays, gene expression profiling and discovery of functional genes. *Poultry Science* 82:939-951
18. **Glass B, Wang X, Carre W, Rejto L, Cogburn LA** 2002 DNA microarray analysis of liver genes during the metabolic jump from choriollantoic to pulmonary respiration. *Poult Sci* 81 (Suppl. 1):31
19. **Wang X, Carre W, Rejto L, Cogburn LA** 2002 Global gene expression profiling in liver of thyroid manipulated and/or growth hormone (GH) injected broiler chickens. *Poult Sci* 81 (Suppl. 1):63
20. **Duclos MJ, Wang X, Carre W, Rejto L, Simon J, Cogburn LA**, Nutritional regulation of global gene expression in chicken liver during fasting and re-feeding. (Abstract)
21. **Wang X, Carre W, Zhou H, Lamont SJ, Cogburn LA** 2004 Duplicated Spot 14 genes in the chicken: characterization and identification of polymorphisms associated with abdominal fat traits. *Gene* 332:79-88

22. **Aggrey S, Ankra-Badu GA, Le Bihan-Duval E, Carre W, Wang X, Pitel F, Vignal A, Beaumont C, Duclos MJ, Simon J, Porter TE, Cogburn LA** 2006 Molecular dissection of fatness and body composition: An integrated approach using genome-wide QTL scan, cDNA microarray analysis and orthologous comparisons. submitted
23. **Lagarrigue S, Pitel F, Carre W, Abasht B, Le Roy P, Neau A, Amigues Y, Sourdioux M, Simon J, Cogburn LA, Aggrey S, Leclercq B, Vignal A, Douaire M** 2006 Mapping quantitative trait loci affecting fatness and breast muscle weight in meat-type chicken lines divergently selected on abdominal fatness. *Genet Sel Evol* 38:85-97
24. **Abasht B, Pitel F, Lagarrigue S, Le Bihan-Duval E, Pascale LR, Demeure O, Vignoles F, Simon J, Cogburn L, Aggrey S, Vignal A, Douaire M** 2006 Fatness QTL on chicken chromosome 5 and interaction with sex. *Genet Sel Evol* (in press):
25. **Glass B, Wang X, Carre W, Rejto L, Cogburn LA** 2002 DNA microarray analysis of liver genes during the metabolic jump from chorioallantoic to pulmonary respiration. *Poult Sci* 81:31-Abstract # 128
26. **Wang M** 2005 The role of glucocorticoid action in the pathophysiology of the metabolic syndrome. *Nutr Metab* 2:1-14
27. **Saadoun A, Simon J, Leclercq B** 1987 Effect of exogenous corticosterone in genetically fat and lean chickens. *Brit Poult Sci* 28:519-528
28. **Simon J** 1984 Effects of daily corticosterone injections upon plasma glucose, insulin, uric acid and electrolytes and food intake pattern in the chicken. *Diabete & Metabolism* 10:211-217
29. **Cogburn LA, Wang X, Carre W, Rejto L, Porter TE, Aggrey SE, Simon J** 2003 Systems-wide chicken DNA microarrays, gene expression profiling and discovery of functional genes. *Poult Sci* 82:939-951
30. **Wang X, Carré W, Rejtö L, Cogburn LA** 2005 Transcriptional profiling in liver of hormonally-manipulated chickens. In: A Dawson and PJ Sharp, ed. *Functional Avian Endocrinology*. New Delhi, India: Narosa Publishing House
31. **Cogburn LA** 1991 Endocrine manipulation of body composition in broiler chickens. *Crit Rev Poult Biol* 3:283-305

32. **Richards MP, Poch SM, Coon CN, Rosebrough RW, Ashwell CM, McMurtry JP** 2003 Feed restriction significantly alters lipogenic gene expression in broiler breeder chickens. *J Nutr* 133:707-715
33. **Ingle-Fehr J, Baxter GM** 1998 Skin preparation and surgical scrub techniques. In: White NA, Moore JN, eds. *Current Techniques in Equine Surgery and Lameness*. 2nd ed. Philadelphia: W.B. Saunders Co.; 68-72
34. **Yang IV, Chen E, Hasseman J, Liang W, Frank B, Wang S, Sharov V, Saeed AI, White J, Li J, Lee HN, Yeatman TJ, Quackenbush J** 2002 Within the fold: assessing differential expression measures and reproducibility in microarray assays. *Genome Biology* 3:
35. **Dombkowski AA, Thibodeau BJ, Starcevic SL, Novak RF** 2004 Gene-specific dye bias in microarray reference designs. *FEBS Letters* 560:120-124
36. **Wolfinger RD, Gibson G, Wolfinger ED, Bennett L, Hamadeh H, Bushel P, Afshari C, Paules RS** 2001 Assessing gene significance from cDNA microarray expression data via mixed models. *J Comput Biol* 8:625-637
37. **Tempelman RJ** 2005 Assessing statistical precision, power, and robustness of alternative experimental designs for two color microarray platforms based on mixed effects models. *Vet Immunol Immunopath* 105:175-186
38. **Pandey R, Guru RK, Mount DW** 2004 Pathway miner: extracting gene association networks from molecular pathways for predicting the biological significance of gene expression microarray data. *Bioinformatics* doi:10.1093/bioinformatics/bth215:
39. **Beale EG, Hammer RE, Antoine B, Forest C** 2004 Disregulated glyceroneogenesis: PCK1 as a candidate diabetes and obesity gene. *Trends Endocrinol Metab* 15:129-135
40. **Towle HC, Kaytor EN, Shih H-M** 1997 Regulation of the expression of lipogenic enzyme genes by carbohydrate. *Annu Rev Nutr* 17:405-433
41. **Dehnhard M, Schreer A, Krone O, Jewgenow K, Krause M, Grossman R** 2003 Measurement of plasma corticosterone and fecal glucocorticoid metabolites in the chicken (*Gallus domesticus*), the great cormorant (*Phalacrocorax carbo*), and the goshawk (*Accipiter gentilis*). *Gen Comp Endocrinol* 131:345-352

42. **Hazelwood RL** 1984 Pancreatic hormones, insulin/glucagon molar ratios, and somatostatin as determinates of avian carbohydrate metabolism. *J Exp Zoology* 232:647-652
43. **Kono T, Nishida M, Nishiki Y, Seki Y, Sato K, Akiba Y** 2005 Characterisation of glucose transporter (GLUT) gene expression in broiler chickens. *Br Poult Sci* 46:510-515
44. **de Martino MU, Bhattachryya N, Alesci S, Ichijo T, Chrousos GP, Kino T** 2004 The glucocorticoid receptor and the orphan nuclear receptor chicken ovalbumin upstream promoter-transcription factor II interact with and mutually affect each other's transcriptional activities: Implications for intermediary metabolism. *Mol Endocrinol* 18:820-833
45. **Prieur X, Huby T, Coste H, Schaap FG, Chapman MJ, Rodriguez JC** 2005 Thyroid Hormone Regulates the Hypotriglyceridemic Gene APOA5. *J Biol Chem* 280:27533-27543
46. **Mao JNC, Burnside J, Postel-Vinay MC, Chambers J, Pesek J, Cogburn LA** 1998 Ontogeny of growth hormone receptor gene expression in tissue of growth-selected strains of broiler chickens. *J Endocrinol* 156:67-75
47. **Parini P, Davis M, Lada AT, Erickson SK, Wright TL, Gustafsson U, Sahlin S, Einarsson C, Eriksson M, Angelin B, Tomoda H, Omura S, Willingham MC, Rudel LL** 2004 ACAT2 is localized to hepatocytes and is the major cholesterol-esterifying enzyme in human liver. *Circulation* 110:2017-2023
48. **Bourneuf E, Herault F, Chicault C, Carre W, Assaf S, Monnier A, Mottier S, Lagarrigue S, Douaire M, Mosser J, Diot C** 2006 Microarray analysis of differential gene expression in the liver of lean and fat chickens. *Gene In Press*, Corrected Proof:
49. **Hiukka A, Fruchart-Najib J, Leinonen E, Hilden H, Fruchart J-C, Taskinen MR** 2005 Alterations of lipids and apolipoprotein CIII in very low density lipoprotein subspecies in type 2 diabetes. *Diabetologia* 48:1207-1215
50. **Smith J, Amri MA, Sniderman AD** 2005 What do we (not) know about apoB, type 2 diabetes and obesity? *Diabetes Research and Clinical Practice* 69:99-101

51. **Chang BH-J, Li L, Paul A, Taniguchi S, Nannegari V, Heird WC, Chan L** 2005 Protection against fatty liver but normal adipogenesis in mice lacking adipose differentiation-related protein. *Mol Cell Biol* 26:1063-1076
52. **Cogburn LA, Morgan R, Burnside J** 2003 Expressed sequence tags, DNA chip technology and gene expression profiling. In: Muir WM, Aggrey SE, eds. *Poultry Genetics, Breeding & Biotechnology*. Wallingford: CABI Publishing; 629-646
53. **Koo S-H, Towle HC** 2000 Glucose regulation of mouse S14 gene expression in hepatocytes. *J Biol Chem* 275:5200-5207
54. **Carre W, Diot C, Fillon V, Crooijmans RPMA, Lagarrigue S, Morrisson M, Vignal A, Groenen MAM, Douaire M** 2001 Development of 112 unique expressed sequence tags from chicken liver using an arbitrarily primed reverse transcriptase-polymerase chain reaction and single strand conformation gel purification method. *Anim Genet* 32:289-297
55. **Miller LD, Park KS, Guo QM, Alkharouf NW, Malek RL, Lee NH, Liu ET, Cheng SY** 2001 Silencing of Wnt signaling and activation of multiple metabolic pathways in response to thyroid hormone-stimulated cell proliferation. *Mol Cell Biol* 21:6626-6639
56. **Tolmasoff JM, Ono T, Cutler RG** 1980 Superoxide dismutase: correlation with life-span and specific metabolic rate in primate species. *Proc Natl Acad Sci (USA)* 77:2777-2781
57. **Tanoue T, Takeichi M** 2005 New insights into Fat cadherins. *J Cell Sci* 118:2347-2353
58. **Cogburn LA, Carré W, Wang X, Rejtő L, Duclos M, Simon J** 2005 Gene expression profiles in liver and abdominal fat during development of broiler chickens divergently selected for either high or low body weight. *Proc Plant Anim Genom XIII Conf*, San Diego, CA
59. **Savon S, Hakimi P, Crawford D, Klemm DJ, Gurney AL, Hanson RW** 1997 The promoter regulatory regions of the genes for the cytosolic form of phosphoenolpyruvate Carboxykinase (GTP) from the chicken and the rat have different species-specific roles in gluconeogenesis. *American Society for Nutritional Resources*
60. **Cao H, Van der Veer E, Ban MR, Hanley AJG, Zinman B, Harris SB, Young TK, Pickering JG, Hegele RA** 2004 Promoter polymorphism in PCK1

(phosphoenolpyruvate carboxykinase gene) associated with type 2 diabetes mellitus. *J Clin Endocrinol & Metab* 89:898-903

61. **Lu Z, Gu Y, Rooney SA** 2001 Transcriptional regulation of the lung fatty acid synthase gene by glucocorticoid, thyroid hormone and transforming growth factor- β 1. *Bioch Biophys Acta* 1532:213-222
62. **Ren B, Thelen A, Peters FJ, Jump DB** 1997 Polyunsaturated fatty acid suppression of hepatic fatty acid synthase and S14 gene expression does not require peroxisome proliferator-activated receptor *alpha*. *J Biol Chem* 272:26827-26832
63. **Stahlberg N, Merino R, Hernandez LH, Fernandez-Perez L, Sandelin A, Engstrom P, Tollet-Egnell P, Lenhard B, Flores-Morales A** 2005 Exploring hepatic hormone actions using a compilation of gene expression profiles. *BMC Physiology* 5:8
64. **Almon RR, Dubois DC, Jin JY, Jusko WJ** 2005 Pharmacogenomic responses of rat liver to methylprednisolone: and approach to mining a rich microarray time series. *The AAPS Journal* 2005 7:E156-E194
65. **Yen PM, Ando S, Feng X, Liu Y, Maruvada P, Xia X** 2006 Thyroid hormone action at the cellular, genomic and target gene levels. *Mol Cell Biol* In Press, Corrected Proof:
66. **Carre W, Bourneuf E, Douaire M, Diot C** 2002 Differential expression and genetic variation of hepatic messenger RNAs from genetically lean and fat chickens. *Gene* 299:235-243
67. **Xiao Y, Hughes AL, Ando J, Matsuda Y, Cheng J-F, Skinner-Noble D, Zhang G** 2004 A genome-wide screen identifies a single β -defensin gene cluster in the chicken: implications for the origin and evolution of mammalian defensins. *BMC Genomics* 5:
68. **Lynn DJ, Higgs R, Gaines S, Tierney J, James T, Lloyd AT, Fares MA, Mulcahy G, O'Farrelly C** 2004 Bioinformatic discovery and initial characterisation of nine novel antimicrobial peptide genes in the chicken. *Immunogenetics* 56:170-177
69. **Patil AA, Cai Y, Sang Y, Blecha F, Zhang G** 2005 Cross-species analysis of the mammalian β -defensin gene family: presence of syntenic gene clusters and preferential expression in the male reproductive tract. *Physiol Genomics* 23:5-17

70. **Lehrer RI, Lichtenstein AK, Ganz T** 1993 Defensins-antimicrobial and cytotoxic peptides of mammalian-cells. *Annual Review of Immunology* 11:105-128
71. **Gallo RI, Murakami M, Ohtake T, Ziaou M** 2002 Biology and clinical relevance of naturally occurring antimicrobial peptides. *Journal of Allergy and Clinical Immunology* 110:823-831
72. **Harder J, Bartels J, Christophers E, Schroder JM** 1997 A peptide antibiotic from human skin. *Nature* 387:861
73. **Boman HG** 1991 Antibacterial peptides-key components needed in immunity. *Cell* 65:205-207
74. **Andreu D, Rivas L** 1998 Animal antimicrobial peptides: An overview. *Biopolymers* 47:415-433
75. **Martin E, Ganz T, Lehrer RI** 1995 Defensins and other endogenous peptide antibiotics of vertebrates. *J Leukocyte Biol* 58:128-136
76. **Evans EW, Beach GG, Wunderlich J, Wunderlich BG** 1994 Isolation of antimicrobial peptides from avian heterophils. *J Leukocyte Biol* 56:661-665
77. **Sugiarto H, Yu PL** 2004 Avian antimicrobial peptides: the defense role of [beta]-defensins. *Biochem Biophys Res Comm* 323:721-727
78. **Semple CAM, Mark R, Dorin JR** 2003 Duplication and selection in the evolution of primate β -defensin genes. *Genome Biol* 4:R31
79. **Arner P** 2003 The adipocyte in insulin resistance: key molecules and the impact of the thiazolidinediones. *Trends Endo Metab* 14:137-141
80. **Neels JG, Olefsky JM** 2006 Inflamed fat: what starts the fire? *J Clin Invest* 116:33-35
81. **Bastard J-P, Mustapha M, Lagathu C, Kim MJ, Caron M, Hubert V, Capeau J, Feve B** 2006 Recent advances in the relationship between obesity, inflammation, and insulin resistance. *Eur Cytokine Netw* 17:4-12
82. **Lee YH, Nair S, Rousseau E, Allison D, Page G, Tataranni P, Bogardus C, Permana P** 2005 Microarray profiling of isolated abdominal subcutaneous adipocytes from obese vs non-obese Pima Indians: increased expression of inflammation-related genes. *Diabetologia* 48:1776-1783

